Cooperation between Rho-GEF Gef2 and its binding partner Nod1 in the regulation of fission yeast cytokinesis

Yi-Hua Zhu[a], Yanfang Ye[a,b,*], Zhengrong Wu[c], and Jian-Qiu Wu[a,b]
[a]Department of Molecular Genetics, [b]Department of Molecular and Cellular Biochemistry, and [c]Department of Chemistry and Biochemistry, The Ohio State University, Columbus, OH 43210

ABSTRACT Cytokinesis is the last step of the cell-division cycle, which requires precise spatial and temporal regulation to ensure genetic stability. Rho guanine nucleotide exchange factors (Rho GEFs) and Rho GTPases are among the key regulators of cytokinesis. We previously found that putative Rho-GEF Gef2 coordinates with Polo kinase Plo1 to control the medial cortical localization of anillin-like protein Mid1 in fission yeast. Here we show that an adaptor protein, Nod1, colocalizes with Gef2 in the contractile ring and its precursor cortical nodes. Like *gef2Δ*, *nod1Δ* has strong genetic interactions with various cytokinesis mutants involved in division-site positioning, suggesting a role of Nod1 in early cytokinesis. We find that Nod1 and Gef2 interact through the C-termini, which is important for their localization. The contractile-ring localization of Nod1 and Gef2 also depends on the interaction between Nod1 and the F-BAR protein Cdc15, where the Nod1/Gef2 complex plays a role in contractile-ring maintenance and affects the septation initiation network. Moreover, Gef2 binds to purified GTPases Rho1, Rho4, and Rho5 in vitro. Taken together, our data indicate that Nod1 and Gef2 function cooperatively in a protein complex to regulate fission yeast cytokinesis.

INTRODUCTION

Cytokinesis is the last step of the cell cycle and is essential for cell proliferation and differentiation. Most proteins and key events in cytokinesis are evolutionarily conserved from fungal to human cells (Pollard and Wu, 2010; Green *et al.*, 2012; Lee *et al.*, 2012; Wloka and Bi, 2012). In the fission yeast *Schizosaccharomyces pombe*, anillin-related protein Mid1 plays a crucial role in early stages of cytokinesis (Chang *et al.*, 1996; Sohrmann *et al.*, 1996; Bähler *et al.*, 1998a; Paoletti and Chang, 2000; Lee and Wu, 2012; Saha and Pollard, 2012a). Mid1 resides in the nucleus and in protein complexes called nodes at the medial cortex during interphase (Bähler *et al.*, 1998a; Paoletti and Chang, 2000; Almonacid *et al.*, 2011). Together with the DYRK kinase Pom1, these medial nodes control cell size and mitotic entry (Martin and Berthelot-Grosjean, 2009; Moseley *et al.*, 2009; Hachet *et al.*, 2011). During G2/M transition, more Mid1 is released from the nucleus to the cortical nodes by Polo kinase Plo1 via phosphorylation of Mid1 (Bähler *et al.*, 1998a; Almonacid *et al.*, 2011). These Mid1 nodes mature into cytokinesis nodes by recruiting other proteins, such as IQGAP Rng2, myosin-II, F-BAR protein Cdc15, and formin Cdc12 (Wu *et al.*, 2003, 2006; Motegi *et al.*, 2004; Almonacid *et al.*, 2011; Laporte *et al.*, 2011; Padmanabhan *et al.*, 2011). Then the nodes and actin filaments condense into a compact ring through a search, capture, pull, and release mechanism (Vavylonis *et al.*, 2008; Chen and Pollard, 2011; Ojkic *et al.*, 2011; Laporte *et al.*, 2012). The compact ring matures and constricts, guiding the formation of a division septum (Pollard and Wu, 2010; Proctor *et al.*, 2012). The cell is then divided into two daughter cells with the degradation of primary septum.

The F-BAR protein Cdc15 is essential for cytokinesis (Fankhauser et al., 1995; Carnahan and Gould, 2003; Roberts-Galbraith et al., 2009, 2010; Arasada and Pollard, 2011). In early cytokinesis, Mid1 recruits Cdc15 to cytokinesis nodes, which in turn recruits the formin Cdc12 to nucleate actin filaments (Carnahan and Gould, 2003; Kovar et al., 2003; Laporte et al., 2011). Cdc15 is also essential for contractile-ring maturation and assembly regulated by the septation initiation network (SIN) pathway (Wachtler et al., 2006; Hachet and Simanis, 2008; Laporte et al., 2012). During late cytokinesis, Cdc15 and another F-BAR protein, Imp2, recruit C2-domain protein Fic1 and paxillin Pxl1 to ensure the maintenance and integrity of the contractile ring (Pinar et al., 2008; Roberts-Galbraith et al., 2009).

The contractile ring and septation/septum formation are regulated by the SIN pathway, which is composed of a GTPase and a kinase cascade (Wachtler et al., 2006; Hachet and Simanis, 2008; Krapp and Simanis, 2008; Johnson et al., 2012). The SIN proteins locate at the spindle pole body (SPB) via scaffold proteins Cdc11 and Sid4 (Chang and Gould, 2000; Krapp et al., 2001; Tomlin et al., 2002; Morrell et al., 2004). SIN pathway signaling is controlled by the activation of the GTPase Spg1 by Polo kinase, and the inactivation by the two component GTPase-activating proteins Cdc16 and Byr4 (Schmidt et al., 1997; Furge et al., 1998, 1999; Jwa and Song, 1998; Tanaka et al., 2001; Krapp et al., 2008). The GTP-bound Spg1 interacts with kinase Cdc7 and causes its redistribution to the new SPB (Fankhauser and Simanis, 1994; Cerutti and Simanis, 1999; Mehta and Gould, 2006). The downstream kinases and their binding partners, including Sid1-Cdc14 and Sid2-Mob1, are then activated and recruited onto the SPB (Fankhauser and Simanis, 1993; Balasubramanian et al., 1998; Sparks et al., 1999; Guertin et al., 2000; Hou et al., 2000; Salimova et al., 2000). Activated Sid2-Mob1 is then relocalized to the contractile ring to promote contractile-ring constriction and septum formation (Jin et al., 2006; Chen et al., 2008)

Besides the equivalents of the SIN pathway, MEN and Hippo pathways, Rho GTPase Rho1/RhoA and its activators, the Rho guanine nucleotide exchange factor (GEF; Ect2, Pebble, etc.) are involved in division-site specification and contractile-ring formation by activating myosin-II and actin assembly in budding yeast and animal cells (Lehner, 1992; Imamura et al., 1997; O'Keefe et al., 2001; Tolliday et al., 2002; Bement et al., 2005; Yuce et al., 2005; Nishimura and Yonemura, 2006; Yoshida et al., 2006; Watanabe et al., 2010; Su et al., 2011). In contrast, Rho GTPases in S. pombe regulate only later stages of cytokinesis and cell polarity (García et al., 2006b; Pérez and Rincón, 2010). Fission yeast has six Rho GTPases (Cdc42 and Rho1-5) and seven Rho GEFs (Gef1-3, Rgf1-3, and Scd1). Cdc42, regulated by Gef1 and Scd1, is essential for cell polarity and morphology (Coll et al., 2003; Hirota et al., 2003; Rincón et al., 2007). Rho-GEFs Rgf1-3 activate Rho1, which is essential for cell-wall synthesis, septum formation, and cell polarization (Tajadura et al., 2004; Morrell-Falvey et al., 2005; Mutoh et al., 2005; García et al., 2006a, 2009; Wu et al., 2010). Rho2 is involved in cell morphology and septum formation by regulating cell wall α-glucan biosynthesis (Calonge et al., 2000). Rho3 regulates exocytosis (Nakano et al., 2002; Wang et al., 2003; Kita et al., 2011). Rho4 controls the secretion of lytic enzymes for septum degradation (Nakano et al., 2003; Santos et al., 2003, 2005). Rho5 is a paralogue of Rho1 and shares similar functions (Nakano et al., 2005; Rincón et al., 2006). GEFs that regulate Rho2-5 GTPases are unknown, except that Rgf1 and Rgf2 might weakly interact with Rho5 (Mutoh et al., 2005).

Recently we and others found that the putative Rho-GEF Gef2 localizes to cortical nodes and coordinates with Polo kinase Plo1 to regulate division-site selection (Moseley et al., 2009; Ye et al., 2012; Guzman-Vendrell et al., 2013). In gef2Δ plo1 double mutants, Mid1

localization to the cortical nodes and the contractile ring is severely affected and the division site is misplaced. In addition, these studies showed that Gef2 interacts with Mid1 N-terminus (Ye et al., 2012; Guzman-Vendrell et al., 2013), which is essential for Mid1 function (Almonacid et al., 2009, 2011; Lee and Wu, 2012). The substrate GTPases for Gef2 and the regulation of Gef2, however, are largely unknown.

Here we show that Nod1 forms a complex with Gef2 to regulate cytokinesis. Nod1 and Gef2 are interdependent for their localization to cortical nodes and the contractile ring. Their localization at the contractile ring also depends on the physical interaction between Nod1 and the F-BAR protein Cdc15. Like gef2Δ, nod1Δ suppresses SIN mutants by reducing cell lysis. In addition, the GEF domain of Gef2 interacts with GTPases Rho1, Rho4, and Rho5 in vitro. Thus it is possible that the Gef2/Nod1 complex may activate and function through Rho GTPases during cytokinesis.

RESULTS

Nod1 is a Gef2-related protein that localizes to cortical nodes and the contractile ring

We previously found that the putative Rho-GEF Gef2 plays a role in division-site positioning in cooperation with Polo kinase, Plo1 (Ye et al., 2012). Concurrently, we identified a novel protein, Nod1 (SPAC12B10.10; Jourdain et al., 2013), in the S. pombe protein database with sequence similarity to Gef2. Nod1 is annotated as a sequence orphan with 419 amino acids (aa; www.pombase.org/spombe/result/SPAC12B10.10). Although it has no GEF domain, Nod1 shares 18% identity and 34% similarity with Gef2 C-terminal aa 636–1101 (Figure 1A). The structure prediction program suggested that Nod1 is a helix-rich protein with no predicted domain (Jones, 1999; Wood et al., 2012).

To determine Nod1's functions, we first tagged Nod1 with monomeric enhanced green fluorescent protein (GFP) at its C-terminus and examined its localization. Of interest, Nod1 colocalized with Gef2 throughout the cell cycle at interphase nodes, cytokinesis nodes, and the contractile ring (Figure 1B). We next counted Nod1 molecule numbers in cells by measuring its global and local fluorescence intensity (Wu and Pollard, 2005; Laporte et al., 2011). In our previous study, we used strain kanMX6-Pgef2-mECitrine-gef2 (JW3825) to measure the intensity of Gef2 (Ye et al., 2012). We found that the kanMX6 cassette in the strain affected Gef2 expression level, similar to N-terminal tagged F-BAR protein Cdc15 (Wu and Pollard, 2005). We therefore used the kanMX6 looped-out mECitrine-gef2 strain (JW4912) to requantify Gef2 molecules globally and locally. The global Gef2 level was one-third in the kan-sensitive strain (JW4912), whereas the local Gef2 concentrations at the contractile ring and cortical nodes were similar to the original data (Ye et al., 2012). Compared to Gef2 (1440 ± 660 molecules/cell, 570 ± 90 molecules at the contractile ring, and 16 ± 5 molecules/interphase node), Nod1 had 1520 ± 700 molecules/cell, 770 ± 150 molecules at the contractile ring, and 15 ± 5 molecules/interphase node (Figure 1C). Thus the ratio of Nod1 to Gef2 in interphase nodes and contractile ring is ~1:1 and 1.35:1, respectively.

We performed fluorescence recovery after photobleaching (FRAP) assays on interphase nodes to determine Nod1 dynamics at the cell cortex. Nod1 fluorescence recovered with a half-time ($t_{1/2}$) of 170 ± 77 s, and the mobile fraction was ~40%, similar to Gef2 ($t_{1/2}$ = 180 ± 85 s, 37% mobile fraction; Figure 1D). This indicates that both Nod1 and Gef2 are relatively stable on the plasma membrane compared with some other cytokinesis proteins (Laporte et al., 2011). Together these data suggested that Nod1 might play a role in cytokinesis together with the putative Rho-GEF Gef2.
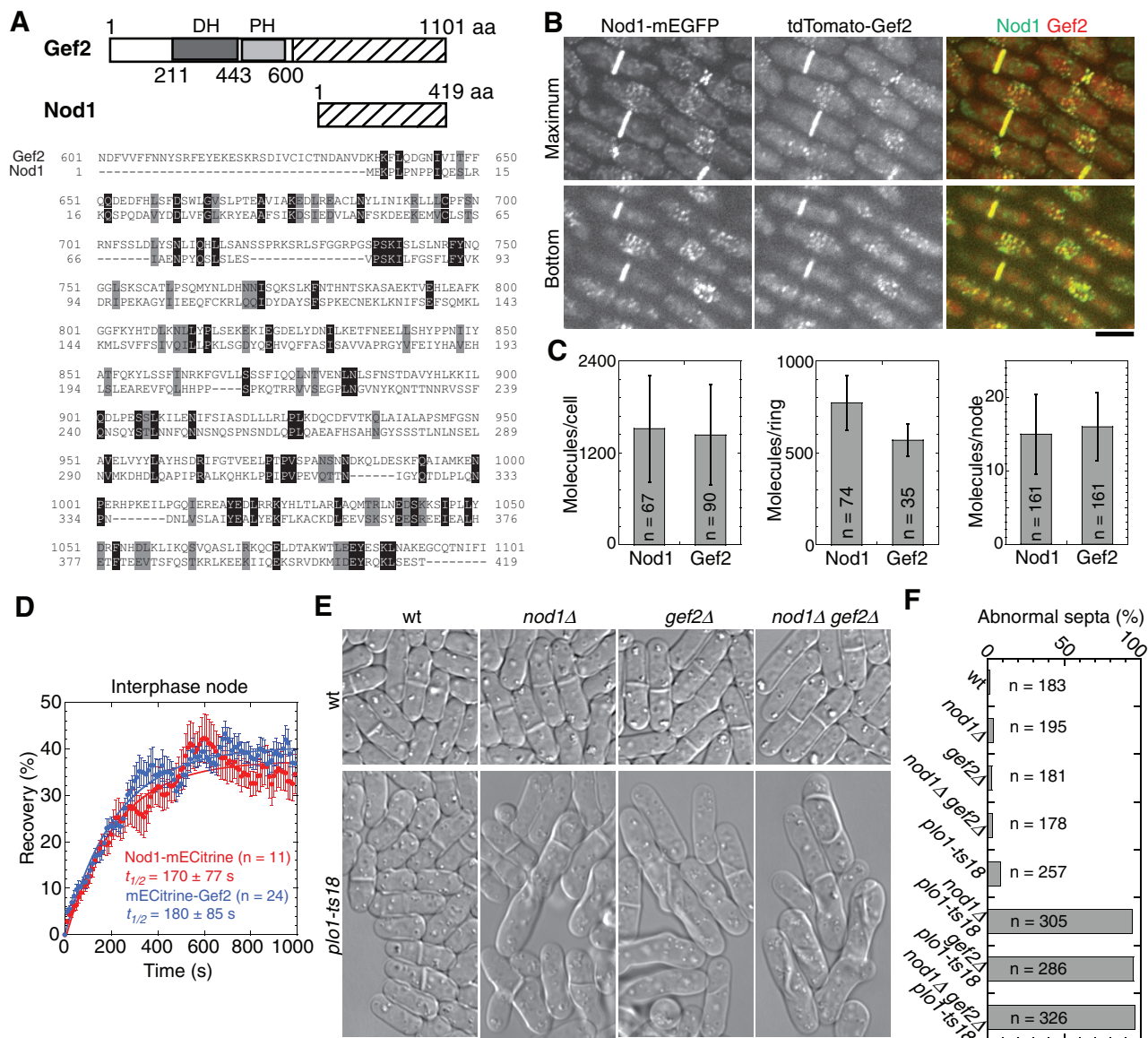
FIGURE 1: Nod1 colocalizes with Gef2 in cortical nodes and the contractile ring and shares similar function with Gef2 in division-site selection. (A) Nod1 shares similarity with Gef2 C-terminus. Top, schematics of Gef2 and Nod1 domains or regions. The similar regions between Nod1 and Gef2 are marked with the same pattern. Bottom, sequence alignment between Gef2 aa 601–1101 (top row) and FL Nod1 (bottom row) using Vector NTI program. Identical and similar (D/E, I/L/V, K/R, N/Q, and S/T) aa are shaded in black and gray, respectively. (B–F) Cells were grown and imaged at 25°C. (B) Colocalization of Nod1 with Gef2 in cortical nodes and the contractile ring (strain JW4457). Top, maximum intensity projection. Bottom, single slice at cell bottom. (C) Molecule numbers of mECitrine-Gef2 (JW4912) and Nod1-mECitrine (JW4008) globally in whole cells and locally in the contractile ring and interphase nodes. (D) FRAP analysis of Nod1 (JW4008) and Gef2 (JW3825). Cells were bleached at time zero. Mean ± SEM. (E, F) Nod1 and Gef2 have similar function in division-site positioning. (E) Differential interference contrast (DIC) images and (F) quantification of the division-site positioning. The abnormal septa are defined as septa not placed within the central 20% of the cell or not within 80–100° angle to the long axis of the cell. Strains used: wt (JW81), nod1Δ (JW3773), gef2Δ (JW1826), nod1Δ gef2Δ (JW3814), plo1-ts18 (IH1600), nod1Δ plo1-ts18 (JW3815), gef2Δ plo1-ts18 (JW3078), and nod1Δ gef2Δ plo1-ts18 (JW3873). Bars, 5 μm.

Nod1 regulates division-site positioning cooperatively with Polo kinase Plo1

Interphase nodes are important for cell-size control and mitotic entry in fission yeast (Martin and Berthelot-Grosjean, 2009; Moseley et al., 2009; Hachet et al., 2011; Deng and Moseley, 2013). As reported (Jourdain et al., 2013), we found that similar to the length of dividing gef2Δ cells (Ye et al., 2012), dividing nod1Δ cells were 16.2 ± 1.0 μm long (n = 148 septating cells), slightly but significantly

longer than 14.4 ± 0.9 μm of wild-type (wt) cells (n = 117, p < 0.001). Thus Nod1 and Gef2 play a role in cell-size control.

Gef2 coordinates with Polo kinase, Plo1, to recruit anillin-related protein Mid1 to the cortical nodes for division-site specification (Ye et al., 2012). Because of the sequence similarity between Nod1 and the C-terminus of Gef2 and their colocalization (Figure 1, A and B), we hypothesized that Nod1 has a function similar to Gef2 at early cytokinesis. To test this hypothesis, we crossed nod1Δ to the
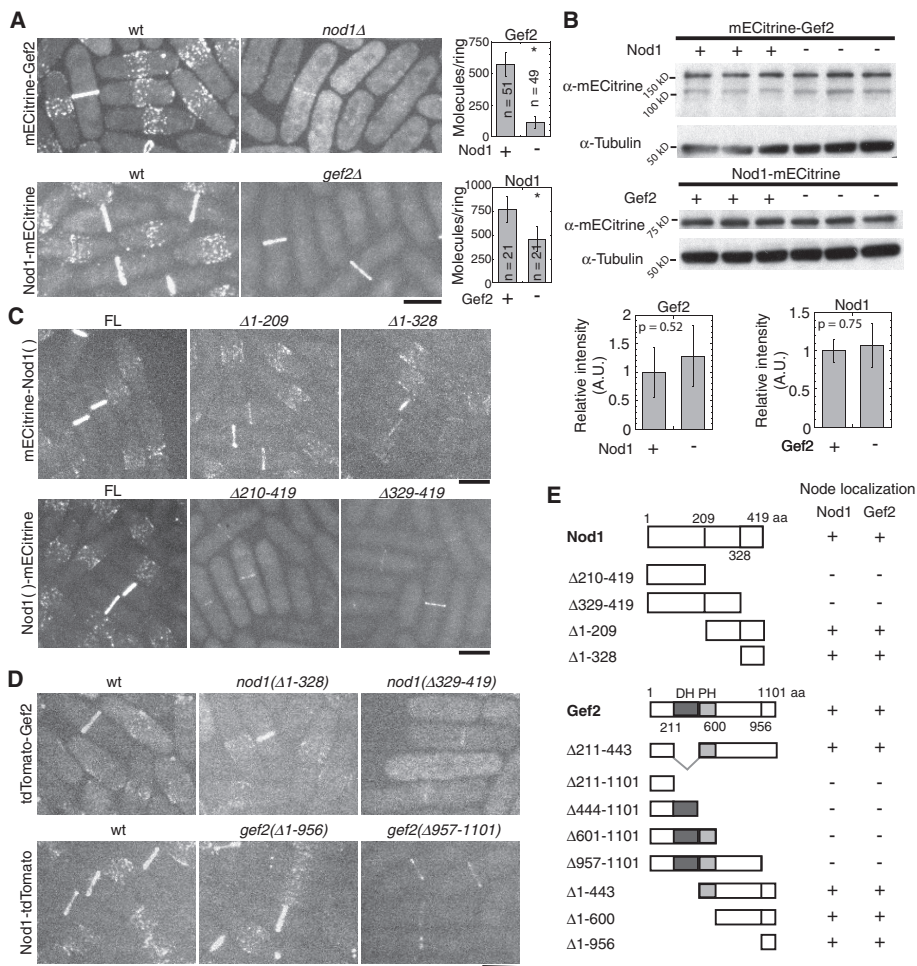
FIGURE 2: Nod1 and Gef2 are interdependent on their C-termini for cortical-node localization and partially interdependent for contractile-ring localization. (A) Micrographs of Nod1 and Gef2 localization in wt and deletion mutants (left). Molecules in the contractile ring were counted (right). Cells expressing mECitrine-Gef2 (JW3825 and JW4014) and Nod1-mECitrine (JW4008 and JW4038) were used. (B) Nod1 and Gef2 protein levels in wt (+) and the deletion (−) mutants. Cells extracts from the strains used in A were loaded in triplicate in Western blotting (top). Tubulin was used as the loading control. The graphs show the quantification of the protein levels (bottom). (C) Micrographs of Nod1 localization in cells expressing mECitrine-tagged FL Nod1 (JW4750 and JW4008) or Nod1 truncations (JW5065, JW4856, JW4325, and JW4326). (D) Micrographs of localization of Nod1 and Gef2 (strains JW4226, JW5107, JW4359, JW4010, JW4256, and JW4355). (E) Summary of Nod1 and Gef2 localization to cortical nodes in different truncation mutants. +, localized to cortical nodes; −, not localized to cortical nodes. Bars, 5 μm.

Nod1 and Gef2 are in the same genetic pathway.

Nod1 and Gef2 are interdependent on their C-termini for localization to cortical nodes

Because Gef2 and Nod1 are in the same genetic pathway, we tested whether they affect each other's localization. In wt cells, Gef2 localized to cortical nodes and the contractile ring (Figure 2A). Node localization was abolished, however, and contractile ring localization was greatly reduced in nod1Δ (Figure 2A). Gef2 was detected at the contractile ring with 115 ± 50 molecules, at ~20% of wt levels, in nod1Δ cells (p < 0.001). Nod1 also failed to localize to cortical nodes in gef2Δ, and the localization to the contractile ring was reduced to ~60% of wt level, with 460 ± 130 molecules (p < 0.001; Figure 2A). The loss of localizations was not due to global protein concentration, since Nod1 and Gef2 protein levels were not significantly affected in the absence of one another (Figure 2B). Thus Gef2 and Nod1 are interdependent for localization to cortical nodes (Jourdain et al., 2013) and partially interdependent for localization to the contractile ring.
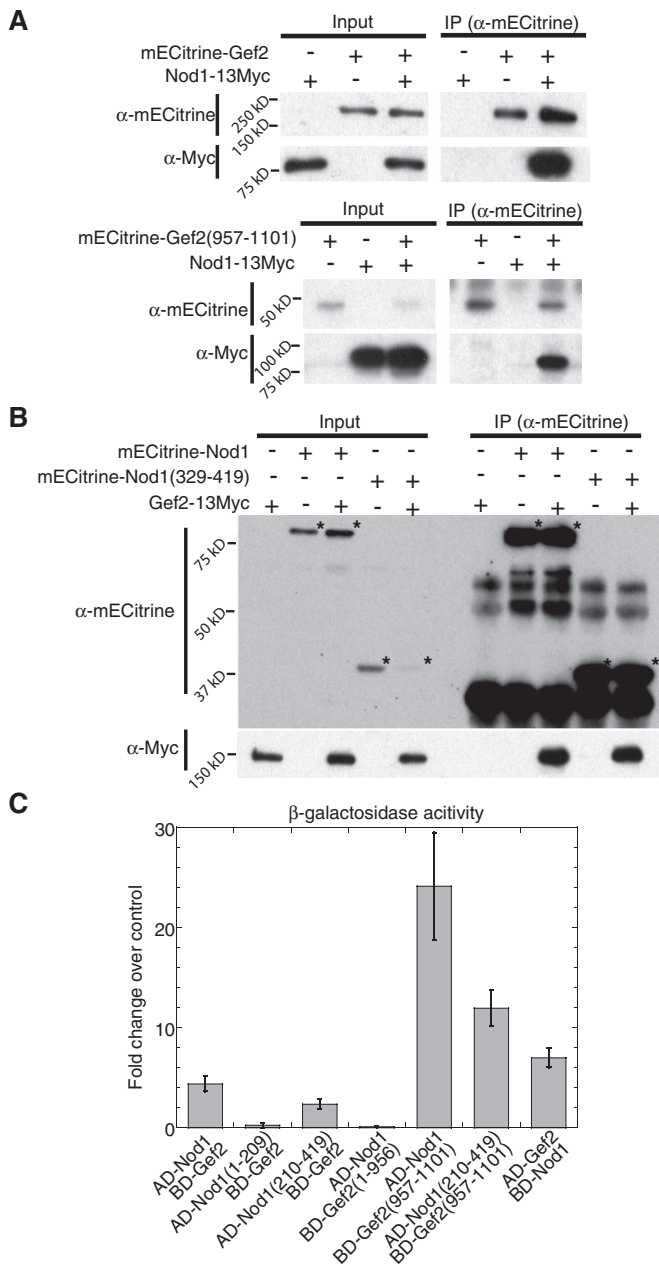
Gef2 C-terminal aa 957–1101 are necessary and sufficient for its cellular localization (Ye et al., 2012). To test which region of Nod1 is important for its localization, we truncated Nod1 at its native chromosomal locus under the control of nod1 promoter based on the sequence alignment between Gef2(601–1101) and Nod1 (Figures 1A and 2E). N-terminal truncations of Nod1 still localized to the cortical nodes and contractile ring (Figure 2C, top). When the last 91 aa of Nod1 from the C-terminus were truncated, however, Nod1 failed to localize to cortical nodes, but it still localized to the contractile ring with lower intensity (Figure 2C, bottom). We conclude that Nod1 C-terminal aa 329–419 are both essential and sufficient for

Nod1 node localization.

Next we studied how the Nod1 and Gef2 truncations affect each other's localization (Figure 2, D and E). Gef2 localized to both cortical nodes and the contractile ring in nod1(Δ1-328) but only localized to the contractile ring weakly when the last 91 aa of Nod1 were truncated in nod1(Δ329-419) (Figure 2D), which is similar to Gef2 localization in nod1Δ (Figure 2A). Similarly, Nod1 localized normally in gef2(Δ1-956) but failed to localize to cortical nodes when Gef2 C-terminal aa 957–1101 were truncated (Figure 2D). Together Nod1 and Gef2 are interdependent on their C-termini for cortical node localization and partially interdependent on their C-termini for localization to the contractile ring (Figure 2E).

Nod1 physically interacts with Gef2 through their C-termini
Based on the interdependence between Nod1 and Gef2 for localization, we hypothesized that the two proteins interact with each

temperature-sensitive mutant of Polo kinase, plo1-ts18 (Figure 1E). Similar to gef2Δ plo1-ts18 (Ye et al., 2012), 95% of nod1Δ plo1-ts18 cells had abnormal septa at 25°C (Figure 1, E and F). Moreover, nod1Δ and gef2Δ also had the same strong synthetic interactions with mutations known to affect early cytokinesis, such as mid1, rng2, and cdc4-8, but not with mutations in cell-size control such as cdr2Δ and blt1Δ (see Table 1 later in the article). Thus Nod1 shares a similar function with Gef2 in division-site specification and contractile-ring assembly (Ye et al., 2012; Jourdain et al., 2013).

To examine whether Nod1 and Gef2 function in the same or parallel genetic pathways, we tested the genetic interactions among nod1Δ, gef2Δ, and plo1-ts18 (Figure 1, E and F). nod1Δ gef2Δ double-mutant cells resembled the single mutants. The nod1Δ gef2Δ plo1-ts18 triple mutant was still viable, with ~96% cells displaying abnormal septa at 25°C, similar to nod1Δ plo1-ts18 and gef2Δ plo1-ts18. These results indicated that

A

Input | IP (α-mECitrine)

mECitrine-Gef2: - + + | - + +
Nod1-13Myc: + - + | + - +

α-mECitrine — 250 kD–, 150 kD–

α-Myc — 75 kD–

Input | IP (α-mECitrine)

mECitrine-Gef2(957-1101): + - + | + - +
Nod1-13Myc: - + + | - + +

α-mECitrine — 50 kD–

α-Myc — 100 kD–, 75 kD–

B

Input | IP (α-mECitrine)

mECitrine-Nod1: - + + - - | - + + - -
mECitrine-Nod1(329-419): - - - + + | - - - + +
Gef2-13Myc: + - + - + | + - + - +

α-mECitrine — 75 kD–, 50 kD–, 37 kD–

α-Myc — 150 kD–

C

β-galactosidase acitivity

Fold change over control (y-axis: 0, 10, 20, 30)

Categories:
AD-Nod1 BD-Gef2
AD-Nod1(1-209) BD-Gef2
AD-Nod1(210-419) BD-Gef2
AD-Nod1 BD-Gef2(1-956)
AD-Nod1 BD-Gef2(957-1101)
AD-Nod1(210-419) BD-Gef2(957-1101)
AD-Gef2 BD-Nod1

FIGURE 3: Nod1 and Gef2 physically interact through their C-termini. (A, B) Antibodies against mECitrine were used in IP. Monoclonal antibodies against mECitrine and Myc were used in Western blotting. (A) Nod1 co-IP with Gef2 C-terminus. IPs were carried out from cell extracts of *nod1-13Myc* (JW4013), *mECitrine-gef2* (JW3825), *mECitrine-gef2 nod1-13Myc* (JW4330), *mECitrine-gef2(957-1101)* (JW3826), *nod1-13Myc* (JW4013), and *mECitrine-gef2(957-1101) nod1-13Myc* (JW4331). (B) Gef2 co-IP with Nod1 C-terminus. Strains JW3622, JW4453, JW5093, JW4455, and JW5095 were used. Asterisks mark the expected bands. (C) Nod1 and Gef2 interact via their C-termini in yeast two-hybrid assays. β-Galactosidase activities (mean ± SD, n = 2) are shown as fold changes over the highest negative control.

other. Indeed, monomeric enhanced Citrine (mECitrine)–Gef2 pulled down Nod1-13Myc in the coimmunoprecipitation (co-IP) assay (Figure 3A). In reciprocal co-IP, mECitrine–Nod1 also pulled down Gef2-13Myc (Figure 3B). Because Nod1 and Gef2 C-termini are important for their localization, we tested whether they interact

through their C-termini. As expected, Nod1 interacted with Gef2(957–1101) (Figure 3A) and Gef2 with Nod1(329–419) (Figure 3B) in co-IP assays. These data suggested that Nod1 and Gef2 interact with each other in vivo through their C-termini.

We tested whether the interaction might be direct between Nod1 and Gef2 through yeast two-hybrid assays (Figure 3C). Full length (FL) Nod1 displayed positive interaction with Gef2 and Gef2(957–1101) but not with Gef2(1–956), whereas FL Gef2 bound to Nod1 and Nod1(210–419) but not to Nod1(1–209). Moreover, Nod1(210–419) interacted with Gef2(957–1101). In summary, Nod1 and Gef2 physically interact with each other through their C-termini, and the interaction is critical for their localization.
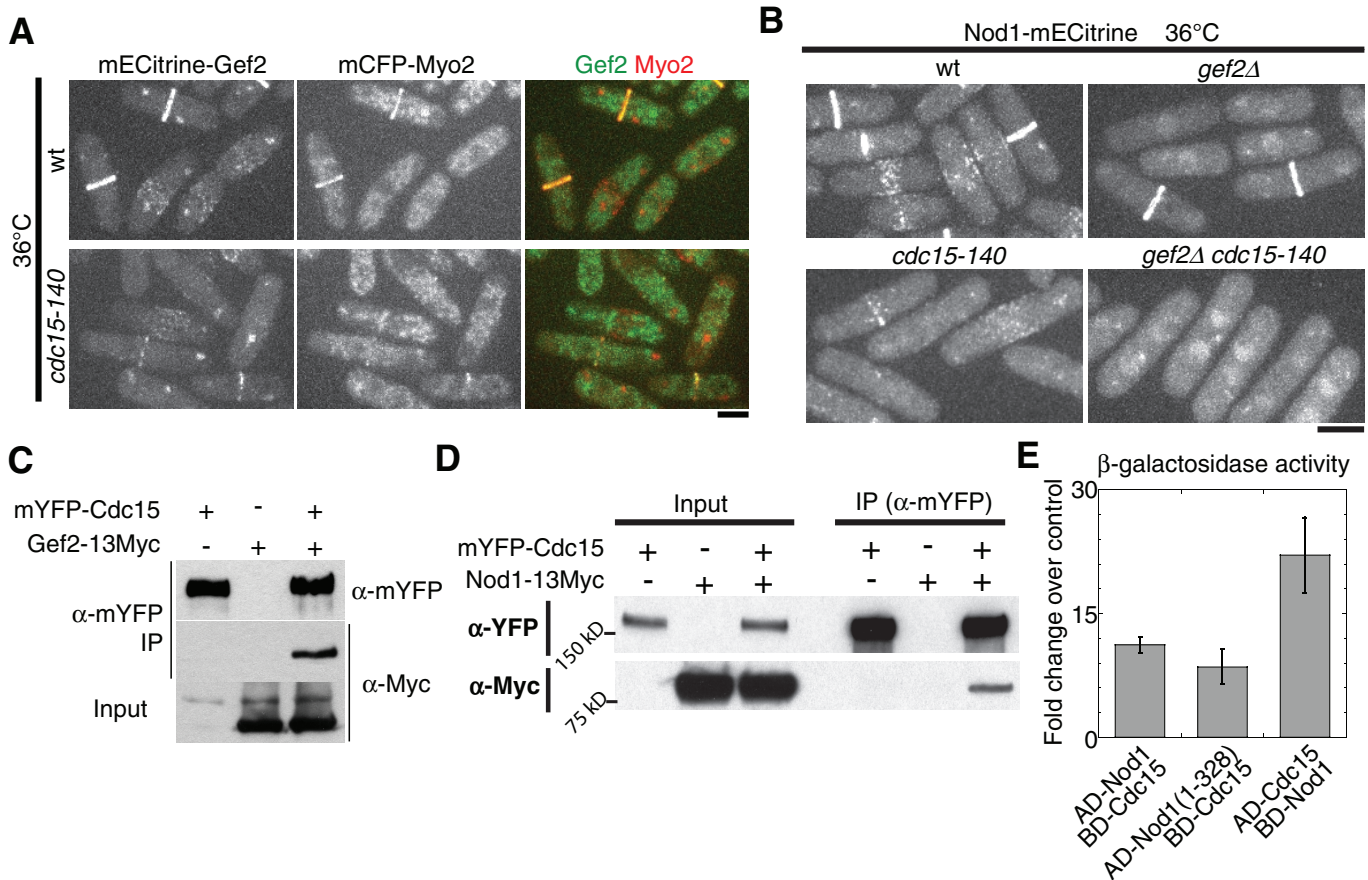
The F-BAR protein Cdc15 recruits Nod1 and Gef2 to the contractile ring through its interaction with the Nod1 N-terminus

Gef2 localizes to cytokinesis nodes and the contractile ring in *blt1Δ*, although interphase-node localization is abolished (Ye et al., 2012). The timings of appearance at cytokinesis nodes for Gef2 in *blt1Δ* and the F-BAR protein Cdc15 in wt cells are similar (Laporte et al., 2011; Ye et al., 2012). Thus we observed Gef2 and Nod1 localization in the temperature-sensitive mutant *cdc15-140* at the restrictive temperature (Figure 4, A and B). After 2 h at 36°C, both Gef2 and Nod1 formed some aggregates, and signals were weaker in *cdc15+* than at 25°C (Figures 2A and 4, A and B). Gef2 and Nod1 still localized to cortical nodes with low intensity, but their contractile-ring localizations were greatly reduced in *cdc15-140* cells (Figure 4, A and B). Unlike in *gef2Δ* cells, the contractile-ring localization of Nod1 was completely abolished in *gef2Δ cdc15-140* cells (Figure 4B). Together our data indicate that the contractile-ring localizations of Nod1 and Gef2 depend on each other and on the F-BAR protein Cdc15.

We next investigated whether Cdc15 physically interacts with Gef2 and Nod1. Monomeric yellow fluorescent protein (mYFP)–Cdc15 pulled down both Gef2-13Myc and Nod1-13Myc from cell lysates in co-IP assays (Figure 4, C and D), suggesting that the three proteins were in a protein complex. Yeast two-hybrid assays revealed no positive interactions between Cdc15 and Gef2, whereas Cdc15 bound to Nod1 and Nod1(1–328) (Figure 4E). This is consistent with our data that Nod1 N-terminal truncations still localize to the contractile ring (Figure 2C). Thus we conclude that the F-BAR protein Cdc15 recruits or stabilizes the Nod1/Gef2 complex to the contractile ring through the N-terminus of Nod1 during mitosis.

Nod1 and Gef2 affect contractile-ring stability during late cytokinesis

The F-BAR protein Cdc15 is an essential component of the contractile ring, which plays multiple roles during early and late cytokinesis (Fankhauser et al., 1995; Roberts-Galbraith et al., 2009, 2010; Laporte et al., 2011). The fact that Cdc15 recruits the Nod1/Gef2 complex to the contractile ring indicated that Nod1 and Gef2 might have additional functions during late cytokinesis besides their role in division-site positioning. Indeed, we found that *nod1Δ* and *gef2Δ* had synthetic genetic interactions with *cdc15-140*. The double mutants *nod1Δ cdc15-140* and *gef2Δ cdc15-140* failed to form colonies, whereas *cdc15-140* mutant still grew at 30°C (Figure 5A; see Table 1 later in the paper). At 25°C, both *cdc15-140* single mutant and the double mutants resembled wt (Figure 5B, top). After 6 h at 30°C, cells proliferated with a mean cell length of 11.9 μm for wt and 17.3 μm for *cdc15-140* cells. In contrast, most *nod1Δ cdc15-140* and *gef2Δ cdc15-140* cells were significantly longer, with mean cell length of 26.5 and 28.3 μm, respectively (Figure 5, B and C). We

FIGURE 4: The F-BAR protein Cdc15 recruits or stabilizes Gef2 and Nod1 localization to the contractile ring by interaction with the Nod1 N-terminus. (A, B) Involvement of Cdc15 in Gef2 and Nod1 localization at the contractile ring. Cells expressing mECitrine-Gef2 (A) and Nod1-mECitrine (B) were cultured at 25°C and shifted to 36°C for 2 h before imaging at 36°C. Myo2 was used to mark the contractile ring in A. Strains used were JW4008, JW4038, JW5027, JW5028, JW5582, and JW5583. (C, D) Cdc15 interacts with Gef2 and Nod1 in co-IPs (similar to Figure 3A). Strains used were JW1063, JW5120, JW4013, JW3325, and JW3204. (E) Cdc15 interacts with Nod1 N-terminus in yeast two-hybrid assays. β-Galactosidase activities (mean ± SD, $n = 2$) as fold changes over the highest negative control are shown. Bars, 5 μm.

next quantified the number of nuclei per cell in these mutants at 30°C (Figure 5D). Wild type had ~13% binucleated cells, whereas cdc15-140 had 24% binucleated cells, and <1% of cells had more than two nuclei. The majority of nod1Δ cdc15-140 and gef2Δ cdc15-140 mutants, however, were binucleated (62 and 58%, respectively), and ~13 and 7% of cells contained more than two nuclei. These results indicated that the synthetic lethality in nod1Δ cdc15-140 and gef2Δ cdc15-140 cells was due to defects in cytokinesis.

To further determine the nature of the defects in nod1Δ cdc15-140 and gef2Δ cdc15-140 cells, we visualized contractile-ring and septum formation in the mutant cells using markers myosin regulatory light chain Rlc1-tandem dimer Tomato (tdTomato) and (1,3)β-D-glucan synthase GFP-Bgs1 (Figure 5E, Supplemental Figure S1, and Supplemental Videos S1–S3). At 36°C, most cdc15-140 mutant cells cannot maintain the contractile ring and form multinucleated cells (Balasubramanian et al., 1998; Wachtler et al., 2006). At a semipermissive temperature of 30°C, Rlc1 localized to the cytokinesis nodes, which coalesced into the contractile ring in most cells. Then Bgs1 left the growing cell tips and accumulated at the contractile ring. The contractile ring constricted, and septum formed (Figure 5E).

Approximately 30% cdc15-140 cells were defective in contractile-ring assembly and stability, however, and the ring eventually collapsed into aggregates (Figure 5, F and G). Consequently, Bgs1 dispersed around the cell cortex, and the cells became elongated and swollen. These defects were more pronounced in nod1Δ cdc15-140 and gef2Δ cdc15-140 cells, for which Rlc1-tdTomato levels at the division site were significantly reduced to ~30% of those in cdc15-140 single mutant (Figure 5, E and G). Approximately 52% of nod1Δ cdc15-140 and gef2Δ cdc15-140 cells failed to maintain the contractile ring (Figure 5, E and F, Supplemental Figure S1, and Supplemental Videos S1–S3). Thus our data suggest that Nod1 and Gef2 help to stabilize the contractile ring.

Nod1 and Gef2 suppress mutants in the SIN pathway and affect Sid2 kinase localization

The SIN pathway regulates contractile-ring maturation, stability, and septum formation (Krapp and Simanis, 2008; Roberts-Galbraith and Gould, 2008). We reported that gef2Δ suppresses cdc11-136 and sid2-250 mutants in the SIN pathway, but the mechanism is unknown (Ye et al., 2012). We tested whether nod1Δ suppressed SIN mutants, using gef2Δ as a control (see Table 1 later in the paper).
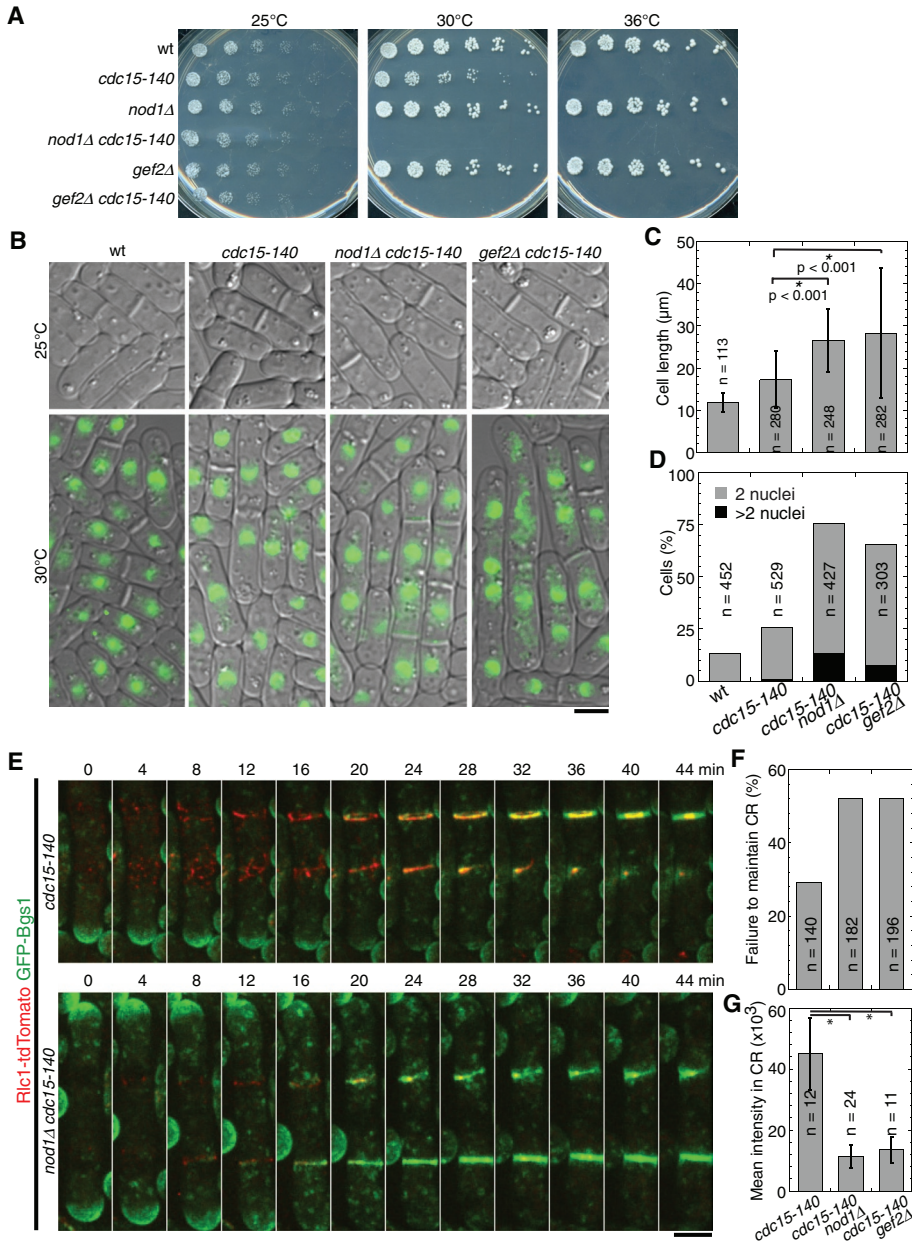
FIGURE 5: Nod1 and Gef2 affect contractile-ring stability. (A) *nod1Δ* and *gef2Δ* display synthetic interaction with *cdc15-140*. Serial dilutions (3×) of indicated strains (JW81, JW1743, JW4259, JW4016, JW2854, and JW2937) on YE5S plates at 25, 30, and 36°C, respectively. (B–D) *nod1Δ cdc15-140* and *gef2Δ cdc15-140* cells display typical cytokinesis defects with elongated and multinucleated cells. Relevant strains used in A were cultured in YE5S liquid at 25° (top) or 30°C (bottom) for 6 h before imaging. (B) Before imaging at 30°C, cells were stained with Hoechst for 10 min at 30°C to visualize DNA (green). DIC in gray. (C) Cell length and (D) number of nuclei in cells grown at 30°C for 6 h. (E–G) Nod1 and Gef2 affect contractile-ring stability during cytokinesis at 30°C. Rlc1 and Bgs1 were used to monitor the contractile ring and septum formation. Cells were grown at 30°C for 6 h before imaging at 30°C. Strains used: JW5357, JW5329, and JW5330. (E) Time courses of selected images from a movie with 1-min delay. The entire series can be viewed in Supplemental Videos S1 and S2. (F) Quantification of cells that fail to maintain the contractile ring (CR) after ring assembly. (G) Mean intensity of Rlc1-tdTomato at CR. Rlc1 intensity is significantly reduced in *nod1Δ cdc15-140* (*p* < 0.001) and *gef2Δ cdc15-140* (*p* < 0.001) cells vs. *cdc15-140* cells. Bars, 5 μm.

Both *gef2Δ* and *nod1Δ* partially restored cell growth of *cdc7-24* at 30°C (Figure 6A, top) and of *cdc11-136* at both 30 and 36°C (Figure 6A, middle). Surprisingly, unlike *gef2Δ*, *nod1Δ* did not suppress *sid2-250* (Figure 6A, bottom; see *Discussion*). To explore the mechanism of the suppression of SIN mutants by *gef2Δ* and *nod1Δ*, we examined cell morphology of SIN single mutants and *SIN gef2Δ* or *SIN nod1Δ* double-mutant cells. *cdc7-24* and *sid2-250* displayed cell lysis (Figure 6B and Supplemental Figure S2). Except for *nod1Δ sid2-250*, all double mutants partially restored cell viability by reducing cell lysis. Approximately 60% *gef2Δ sid2-250* cells survived at a semipermissive temperature of 30°C, whereas only ~20% *sid2-250* and *nod1Δ sid2-250* cells were viable (Figure 6C). On the other hand, cells overexpressing Gef2 from *3nmt1* or *41nmt1* promoter under inducing conditions were synthetic lethal with *sid2-250* at 30°C and synthetic sick with *sid2-1* from 30 to 36°C (Figure 6D). Taken together, our data suggest that both Nod1 and Gef2 negatively affect the SIN pathway or the process regulated by the pathway.

We next tested whether Sid2 localization is affected in *gef2Δ* and *nod1Δ*. Sid2 localizes to the SPB, the contractile ring, and the septum during cytokinesis (Sparks et al., 1999). Sid2 appeared at the contractile ring at the beginning of anaphase B, and the level gradually increased until the contractile ring started to constrict (Figure 6, E, top row, and F) as reported (Sparks et al., 1999; Tebbs and Pollard, 2013). In *gef2Δ* and *nod1Δ*, Sid2 appeared at the contractile ring at a similar timing as in wt. Recruitment of Sid2 to the division site, however, was defective. By the end of anaphase B, Sid2 intensity at the division site in *gef2Δ* and *nod1Δ* was only ~20% of that in wt (Figure 6, E, middle and lower rows, and F; *p* < 0.001 for both *gef2Δ* and *nod1Δ* vs. wt). Moreover, the peak level of Sid2 at the division site in *gef2Δ* and *nod1Δ* was reduced to 57 and 46% that of wt (Figure 6F; *p* < 0.005 for both *gef2Δ* and *nod1Δ* vs. wt). Both wt and mutant cells expressing Sid2-GFP spent more time in mitosis. Because Sid2 regulates proper spindle elongation during anaphase (Mana-Capelli et al., 2012), it seems that Sid2-GFP may not be fully functional. Together these data suggest that Gef2 and Nod1 play a role in recruiting Sid2 to the contractile ring.

Gef2 interacts with Rho GTPases in vitro and is involved in Rho4 localization

Rho GTPases regulate contractile-ring formation, septum formation, and degradation during cytokinesis (Arellano et al., 1997; Nakano et al., 1997, 2003, 2005; Tolliday et al., 2002; Santos et al., 2003; Tajadura et al., 2004; Mutoh et al., 2005; Yoshida et al., 2006). To further dissect the role of Gef2, we tested the interactions
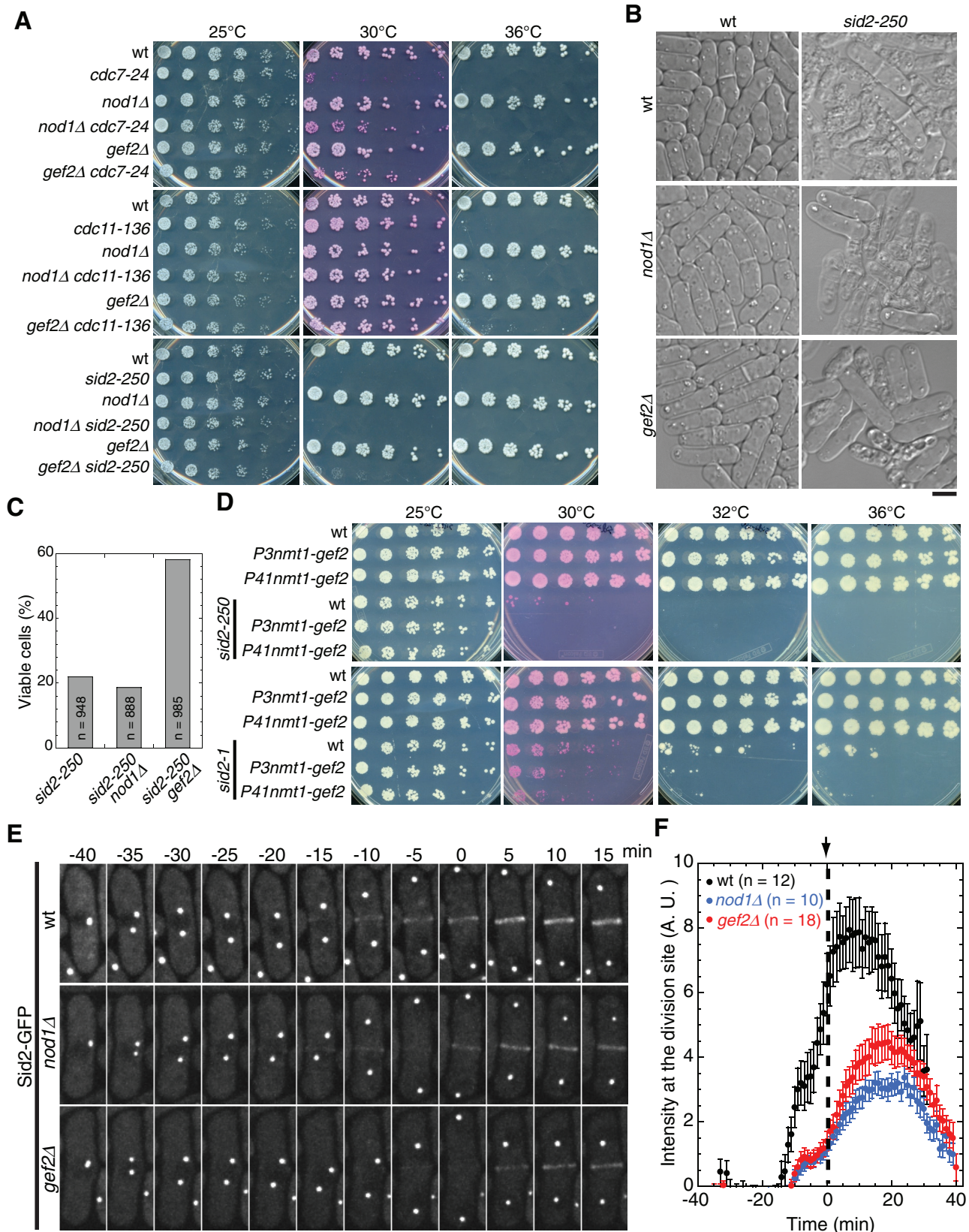
FIGURE 6: *nod1Δ* and *gef2Δ* suppress SIN mutants by reducing cell lysis. (A) Serial dilutions (3×) of indicated strains on YE5S or YE5S + phloxin B (red dye accumulated in dead cells) plates at 25, 30, and 36°C. Strains used: wt (JW81), *cdc7-24* (TP34), *nod1Δ* (JW4259), *nod1Δ cdc7-24* (JW4304), *gef2Δ* (JW2854), *gef2Δ cdc7-24* (JW3021), *cdc11-136* (TP47), *nod1Δ cdc11-136* (JW4306), *gef2Δ cdc11-136* (JW2972), *sid2-250* (YDM429), *nod1Δ sid2-250* (JW4294), and *gef2Δ sid2-250* (JW3009). (B, C) *gef2Δ* but not *nod1Δ* partially rescued cell lysis in *sid2-250*. Cells were grown in liquid culture at 25°C and then shifted 30°C for 6 h. (B) DIC images of *sid2* mutant strains used in A. (C) Percentage of viable cells. Dead or lysed
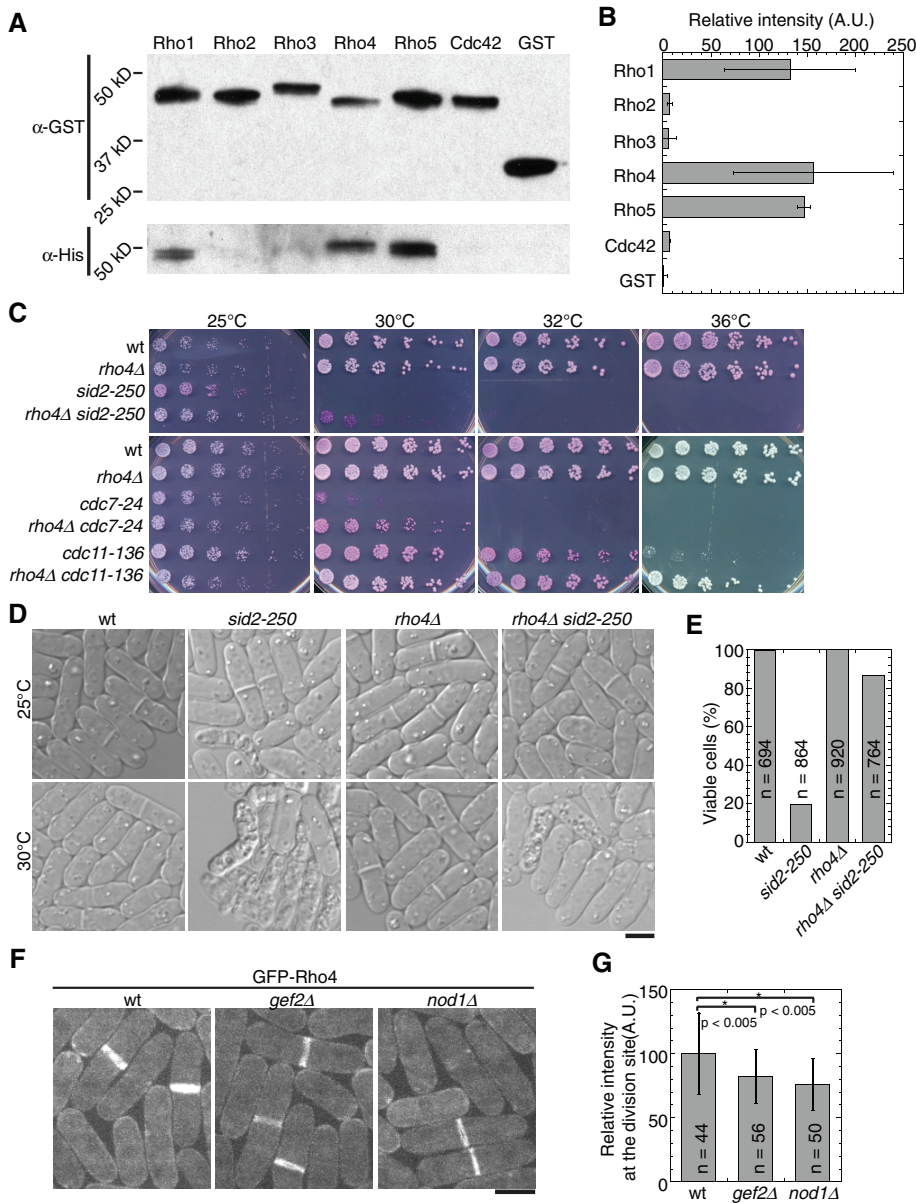
FIGURE 7: Gef2 GEF domain binds to GTPases Rho1, Rho4, and Rho5 in vitro. (A, B) Purified GST-Rho GTPases and GST control were bound to the beads and then incubated with purified His-GEF domain (aa 211–600) of Gef2. The amount of pulled down Gef2 was detected by Western blotting (A) and quantified (B). The intensities of His-Gef2(GEF) bands were measured, background subtracted, corrected for Rho GTPase amount, and normalized by setting the intensity of His-Gef2(GEF) in GST control as 1. The experiment was repeated, and mean ± SD is shown in B. (C–E) rho4Δ suppresses SIN mutants. Strains used: JW81, JW3041, YDM429, JW5505, TP34, JW5503, TP47, and JW5504. (C) Serial dilutions (3×) of indicated strains on YE5S or YE5S + phloxin B plates at 25, 30, 32, and 36°C for 3 d. (D, E) rho4Δ rescues the cell-lysis phenotype of sid2-250. (D) DIC images of cells grown in liquid culture at 25°C or after 6 h at 30°C. (E) Quantification of viable (not lysed or dead) cells after 6 h at 30°C. (F, G) Gef2 and Nod1 play a role in Rho4 localization. (F) Micrographs of GFP-Rho4 in wt (PPG1580) and the deletion mutants (JW4909 and JW4910). (G) Quantification of Rho4 intensity at the division site for strains in (F). Bars, 5 μm.

between the GEF domain of Gef2 and all six Rho GTPases from *S. pombe*. The hexahistidine (6His)-tagged GEF domain (aa 211–600) of Gef2 consisting of the DBL homology (DH) and pleckstrin homology (PH) domains was purified from *Escherichia coli*. The purified GEF domain was then pulled down by purified glutathione *S*-transferase (GST)–tagged Rho proteins. We found that Gef2 interacted with Rho1, Rho4, and Rho5 but not with Rho2, Rho3, and Cdc42 in the pull-down assays (Figure 7, A and B).

To investigate whether Gef2 might function through a Rho GTPase in vivo, we crossed *rho4Δ* to mutants in the SIN pathway, since *rho4Δ*, like *gef2Δ*, has been shown to suppress *sid2-250* (Jin et al., 2006). We found that in addition to rescuing *sid2-250* at both 25 and 30°C, *rho4Δ* also partially rescued *cdc7-24* at 30°C and *cdc11-136* at 30–36°C (Figure 7C). We next observed the cell morphology of *rho4Δ sid2-250* at 25°C or after 6 h at 30°C (Figure 7D). At 25°C, both *rho4Δ* and *rho4Δ sid2-250* resembled wt, whereas *sid2-250* displayed slight cell lysis. At 30°C, only ~20% *sid2-250* cells were viable, whereas ~85% cells survived in *rho4Δ sid2-250* double mutant (Figure 7E). Thus *rho4Δ* resembled *gef2Δ* (Figure 6, A–C) in the suppression of the SIN mutants. Together these data suggest that Gef2 functions through Rho4 GTPase to regulate late cytokinesis.

We next determined whether Gef2 or Nod1 affect Rho4 localization. GFP-Rho4 localized to the cell-division site, as well as to the cell periphery, in wt cells (Nakano et al., 2003; Santos et al., 2003). Although its localization was not abolished, Rho4 intensity at the division site was reduced to 82 and 75% of wt level in *gef2Δ* and *nod1Δ*, respectively (Figure 7, F and G; p < 0.005 for both *gef2Δ* and *nod1Δ* vs. wt). Thus Gef2 and Nod1 are involved in concentrating Rho4 GTPase to the division site during cytokinesis.

DISCUSSION

In this study we found that Nod1, a new player in cytokinesis, regulates division-site positioning and contractile-ring stability together with the putative Rho-GEF Gef2 (Figure 8). In addition, we identified the potential Rho GTPase substrates for Gef2,

cells were identified as those that failed to maintain their cytoplasm. (D) Overexpression of Gef2 is synthetic lethal with *sid2* mutants. Serial dilutions (3×) of indicated strains on YE5S or YE5S + phloxin B plates at 25, 30, and 36°C. Strains used: JW81, JW3561, JW3562, YDM429, JW5360, JW5361, VS2367, JW5405, and JW5406. (E, F) Sid2 localization at the division site is compromised in *nod1Δ* and *gef2Δ*. Time 0 marks the end of anaphase B. (E) Time courses of representative cells expressing Sid2-GFP in wt (YDM415), *gef2Δ* (JW5580), and *nod1Δ* (JW5581). (F) Quantification of the intensity (mean ± SEM) of Sid2-GFP at the division site for strains in E. Black arrow and dashed line mark time 0. Bars, 5 μm.
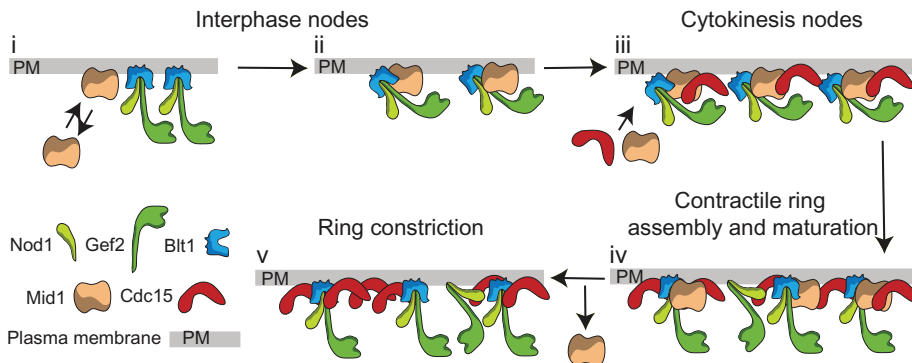
FIGURE 8: Model of Nod1 and Gef2 localization and interactions with other proteins on the cytoplasmic side of the plasma membrane during the cell cycle. i) During interphase, Nod1 and Gef2 localize to interphase nodes via Blt1 or other interphase-node proteins, ii) where they help to recruit and stabilize anillin-related protein Mid1. iii) The nodes mature into cytokinesis nodes and coalesce into the contractile ring as more Mid1 and other cytokinesis proteins like F-BAR protein Cdc15 arrive at the division site. iv) Cdc15 continuously recruits or stabilize the Nod1/Gef2 complex during ring maturation, which helps to maintain the contractile-ring integrity and stability. v) Mid1 disappears from the ring at the onset of its constriction. For clarity, the potential interactions between Gef2 and Rho GTPases are not shown.

suggesting the possible involvement of Gef2 GEF activity and Rho GTPases in the regulation of cytokinesis.

The roles of Rho GTPases during cytokinesis

Among the seven Rho GEFs in *S. pombe*, Gef2 and Gef3 have no identified Rho substrates. We find that Gef2 interacts with Rho1, Rho4, and Rho5 in vitro (Figure 7, A and B). It is unclear whether Gef2 interacts with and activates these Rho GTPases in vivo, but these data provide insight into Gef2's functions as a potential Rho GEF. In previous study, we reported that deletion of Gef2 DH domain causes defects in division-site positioning in ~50% *plo1-ts18* mutant cells at 25°C (Ye *et al.*, 2012). Therefore it is possible that the GEF activity of Gef2 is involved in division-site placement. Rho1 regulates cell integrity and septum formation during late cytokinesis in fission yeast (Nakano *et al.*, 1997; Mutoh *et al.*, 2005). Its homologues RhoA or Rho1 in animal cells and budding yeast, however, are active in early cytokinesis for division-site selection and contractile-ring assembly (Imamura *et al.*, 1997; Tolliday *et al.*, 2002; Bement *et al.*, 2005; Piekny *et al.*, 2005; Yoshida *et al.*, 2006; Watanabe *et al.*, 2010). The presence and function of Gef2 in the cortical nodes might suggest a role of Rho1 during early cytokinesis if Gef2 indeed activates Rho1 in vivo. One difficulty in studying RhoA or Rho1, however, is that its native concentration is low, and therefore it is difficult to detect Rho1 at the division site during early cytokinesis by fluorescence microscopy. Whether Rho1 participates in division-site positioning in fission yeast remains to be tested, and we cannot rule out the possibility that other Rho candidates are also involved.

Of the six Rho GTPases in fission yeast, Rho1 and Cdc42 are relatively well studied, whereas our knowledge on Rho2-5 is limited. For example, no Rho GEFs have been assigned to Rho2, Rho3, and Rho4. Rho4 affects the localization and activity of β-glucanase Eng1 and α-glucanase Agn1, which results in cell separation defects (Nakano *et al.*, 2003; Santos *et al.*, 2003, 2005). Rho5 is a Rho1 paralogue that shares similar functions (Nakano *et al.*, 2005). How Rho4 and Rho5 are regulated and localized is unknown. Our data suggest that Gef2 might be a GEF for Rho4 or Rho5 and help recruit Rho4 to the division site. Rho4 localization, however, is only partially dependent on Gef2 (Figure 7, F and G). More efforts are needed to investigate whether and how Gef2 works with these Rho GTPases.

Localization of Nod1 and Gef2 during the cell cycle

We and others found that Gef2 coordinates with Polo kinase, Plo1, to recruit anillin-like protein Mid1 to the cortical nodes during G2/M transition (Ye *et al.*, 2012; Guzman-Vendrell *et al.*, 2013; Jourdain *et al.*, 2013). During the course of that study, we identified Nod1 as a Gef2-related protein and binding partner. We found that Gef2 and Nod1 form a complex, which is important for their cortical node localization and functions. These results are consistent with a recent report on Nod1 (Jourdain *et al.*, 2013). Gef2 and Nod1 are stable in interphase nodes, as revealed by FRAP assays. Besides a GEF (DH-PH) domain, Gef2 has no other known structures or motifs (Figure 1A; Iwaki *et al.*, 2003). Blt1 was reported to recruit Gef2 to the interphase nodes (Ye *et al.*, 2012; Guzman-Vendrell *et al.*, 2013; Jourdain *et al.*, 2013). It is likely that Blt1 interacts with Nod1 and Gef2 through their C-termini (Figure 8). Both Nod1 and Gef2 have enriched α-helix structures at C-termini (Jones, 1999). Gef2 still localizes to cytokinesis nodes in *blt1Δ*, so Gef2 must have other binding partners during early mitosis. We previously showed that Gef2 interacts with Mid1(300–350) in vivo (Ye *et al.*, 2012). Although we found that Mid1(1–580), which includes the Gef2-binding region, depended on Gef2 C-terminus for node localization, no positive interactions were observed between Mid1(300–350) and several regions of Gef2 or Nod1 in yeast two-hybrid assays (unpublished data). Thus the interactions between Gef2 and Mid1 may be indirect.

Although the majority of Gef2 is recruited to the contractile ring through the cortical nodes, our localization dependence data reveal that both Nod1 and Gef2 are capable of localizing to the contractile ring without each other. We find that F-BAR protein Cdc15 physically interacts with Nod1 and recruits Nod1 to the contractile ring (Figures 4 and 8). Cdc15 appears at cytokinesis nodes ~5 min before SPB separation and is continuously recruited to the contractile ring during mitosis (Wu and Pollard, 2005; Laporte *et al.*, 2011). Consistently, the contractile ring contains ~40% more molecules of Nod1 than Gef2 (Figure 1C). Nod1 intensity at the contractile ring in *gef2Δ* also increases during ring maturation at late mitosis. Without Nod1, Gef2 can still localize to the division site during later stages of cytokinesis (Figure 2A), although Gef2 does not interact with Cdc15 in yeast two-hybrid assays. It is possible that Gef2 depends on alternative mechanisms to localize. One attractive candidate is a Rho GTPase. We found that Gef2 can interact with Rho1, Rho4, and Rho5, and all of them localize to the division site at late cytokinesis (Nakano *et al.*, 2003, 2005; Santos *et al.*, 2003; Mutoh *et al.*, 2005). In budding yeast, activated Cdc42 recruits the Rho-GEF Cdc24 and scaffold protein Bem1 to activate more Cdc42 and establish cell polarity (Butty *et al.*, 2002; Slaughter *et al.*, 2009; Bi and Park, 2012). It is possible that Gef2 and its Rho substrates are involved in a similar positive feedback loop to regulate cytokinesis.

Nod1 and Gef2 coordinate with F-BAR protein Cdc15 to maintain contractile-ring stability

Cdc15 has multiple functions during cytokinesis. During early cytokinesis, Cdc15 recruits the formin Cdc12 to promote contractile-ring assembly (Carnahan and Gould, 2003; Kovar *et al.*, 2003;

Strain	Temperature (°C)[a]				gef2Δ[b]
	25	30	32	36	
plo1-ts18	+++	++	++	+	Same
plo1-ts18 nod1Δ	+	+	+	+/-	
mid1-6	+++	+++	+++	++	Same
mid1-6 nod1Δ	+++	++	++	++	
mid1-366	+++	+++	+++	++	Same
mid1-366 nod1Δ	+	+	+	+	
rng2-D5	+++	++	++	-	Same
rng2-D5 nod1Δ	++	+	+	-	
rng2-346	+++	++	++	-	Same
rng2-346 nod1Δ	++	+	+	-	
cdc4-8	+++	++	++	-	Same
cdc4-8 nod1Δ	+++	+	+	-	
cdc15-140	+++	+	-	-	Same
cdc15-140 nod1Δ	+++	-	-	-	
cdr2Δ	+++	+++	+++	+++	Same
cdr2Δ nod1Δ	+++	+++	+++	+++	
blt1Δ	+++	+++	+++	+++	Same
blt1Δ nod1Δ	+++	+++	+++	+++	
klp8Δ	+++	+++	+++	+++	Same
klp8Δ nod1Δ	+++	+++	+++	+++	
cdc7-24	+++	+	-	-	Same
cdc7-24 nod1Δ	+++	++	-	-	
cdc11-136	+++	++	++	-	Same
cdc11-136 nod1Δ	+++	+++	+++	+/-	
sid2-250	++	-	-	-	Different
sid2-250 nod1Δ	++	-	-	-	
sid2-250 gef2Δ	++	+/-	-	-	

[a]Growth and color of colonies on YE5S + phloxin B plates at various temperatures. +++, similar to wt; ++, mild defects or cell lysis; +, cell lysis with reduced growth rate; +/-, severe cell lysis and slow growth; -, inviable.
[b]The genetic interactions of nod1Δ were compared with those of gef2Δ with corresponding mutants.

TABLE 1: Genetic interactions of nod1Δ with other mutations affecting cytokinesis and cell-size control.

Laporte et al., 2011). During ring maturation at anaphase, Cdc15, together with the SIN pathway and the F-BAR protein Imp2, is believed to be important for maintaining contractile-ring stability and integrity (Wachtler et al., 2006; Hachet and Simanis, 2008; Huang et al., 2008; Roberts-Galbraith et al., 2009). The exact mechanism remains elusive.

Here we add another layer of complexity to the function of Cdc15 during late cytokinesis. In nod1Δ cdc15-140 and gef2Δ cdc15-140, most cells form a fragile contractile ring and become elongated and multinucleated (Figure 5). The severely reduced level of the myosin regulatory light chain Rlc1 suggests loss of proteins from the contractile ring (Figure 5, E–G, Supplemental Figure S1, and Supplemental Videos S1–S3). One possible explanation could

be related to the scaffolding protein Mid1. Mid1 is anchored to the equatorial cortex through the cooperation of its own lipid-binding domains and other cytokinesis proteins, including Cdr2, Gef2, and Blt1 (Almonacid et al., 2009; Lee and Wu, 2012; Ye et al., 2012; Guzman-Vendrell et al., 2013). Mid1 is more dynamic and mobile at the division site without Gef2 (Ye et al., 2012). As a result, the recruitment and maintenance of the contractile-ring components might be less effective during late mitosis, which aggravates the cdc15-mutant phenotype. It is also possible that Rho1 and/or Rho5 GTPases are also involved in contractile-ring stability and their activities are compromised in nod1Δ and gef2Δ cells. Further experiments are needed to distinguish these possibilities.

Nod1 and Gef2 suppress the SIN pathway
The SIN pathway includes a small GTPase and several protein kinases and their adaptors, which form a kinase cascade on the SPB (Fankhauser and Simanis, 1993, 1994; Furge et al., 1998, 1999; Sparks et al., 1999; Chang and Gould, 2000; Guertin et al., 2000; Hou et al., 2000; Salimova et al., 2000; Tomlin et al., 2002). The activation of SIN pathway leads to contractile-ring constriction and septum formation (Wachtler et al., 2006; Hachet and Simanis, 2008; Krapp and Simanis, 2008; Johnson et al., 2012). This is executed by translocation of kinase Sid2 and its adaptor Mob1 from the SPB to the contractile ring (Sparks et al., 1999; Hou et al., 2000; Chen et al., 2008). Discoveries of suppressors of SIN pathway mutants, especially those of sid2, have helped us understand how SIN pathway regulates cytokinesis (Jiang and Hallberg, 2001; Jin and McCollum, 2003; Jin et al., 2006; Goyal and Simanis, 2012). Here we found that nod1Δ and gef2Δ suppress the SIN mutants by improving cell survival at the semipermissive temperature, whereas single-SIN-mutant cells lyse when trying to separate with defective septa (Figure 6, A–C, and Table 1). We also observed that Sid2 accumulation at the division site is delayed and compromised in nod1Δ and gef2Δ cells (Figure 6, E and F). Similar results were observed in IQGAP rng2 without the IQ motifs (Tebbs and Pollard, 2013), suggesting a requirement of intact contractile ring for Sid2 stable localization. Therefore the contractile ring components, including Gef2 and Nod1, may regulate the SIN pathway through direct or indirect influence on contractile-ring localization of Sid2. It is still possible, however, that the defects caused by nod1Δ and gef2Δ affect the rates of contractile-ring maturation and constriction, allowing more time for septum synthesis. Consistently, increasing the amount and activity of β-glucan synthase Bgs1 by overexpressing Rho1 GTPase or its GEF Rgf3 can rescue sid2 mutants (Jin et al., 2006).

Rho4 GTPase, however, might be also involved in the suppression of sid2-250 by gef2Δ. We found that Gef2 binds to Rho4 in vitro. Of interest, deletion of rho4 or its effector eng1 or agn1 partially suppresses sid2-250 (Jin et al., 2006), which is consistent with our results (Figure 7C–E). Thus it is likely that suppression of SIN mutants by gef2Δ is due to a reduced function of Rho4 and its effectors. Consistently, we found that Rho4 localization to the division site was slightly but significantly reduced in both nod1Δ and gef2Δ cells (Figure 7, F and G). This suggests that Gef2 and Nod1 contribute to Rho4 localization besides the undefined role of Rho4 activation. The cell-separation defect of rho4Δ is mild even at 36°C (Santos et al., 2003), suggesting that other mechanisms and pathways are involved in septum degradation. Further studies are needed to identify the redundant pathways.

In conclusion, we find that the Nod1/Gef2 complex functions in division-site positioning, contractile-ring maintenance, and septation besides its role in cell-size control. We also discover the potential Rho GTPase substrates for Gef2. It will be very informative to

investigate whether Gef2 has GEF activity toward the Rho GTPase candidates and whether Nod1 affects Gef2 activity in addition to its localization.

MATERIALS AND METHODS

Strains and genetic, molecular, and cellular methods

Table 2 lists the strains used in this study. We used PCR-based gene targeting and standard yeast genetics to construct strains (Moreno et al., 1991; Bähler et al., 1998b). All tagged and truncation strains are regulated under endogenous promoters or 5' untranslated region (UTR) and integrated into native chromosomal loci, except for the overexpression strains that are integrated at native loci under the control of 3nmt1 or 41nmt1 promoter, which is repressed by thiamine (Maundrell, 1990).

Nod1 C-terminal truncations and Nod1 overexpression were constructed as previously described (Bähler et al., 1998b). For N-terminal truncations, nod1 5' UTR −300 to +3 base pairs was cloned into pFA6a-kanMX6-P3nmt1-mECitrine at BglII and PacI sites to replace the 3nmt1 promoter. The resulting plasmid (JQW560) was then used as the template for PCR amplification and gene targeting. Primers were designed according to desired truncation sites, and

the PCR products were transformed into wt cells. The resulting strains were sequenced. Some kanMX6 marker at 5' end of nod1 or gef2 gene was looped out by crossing the strains to wt cells.

To test the functionalities of tagged FL Nod1, both N- and C-terminally tagged Nod1 strains were crossed to plo1-ts18. Double mutants had <10% abnormal septa at 25°C, which is similar to plo1-ts18 single mutant but different from the ~95% abnormal septa in plo1-ts18 nod1Δ. Thus both N- and C-terminally tagged Nod1 are functional.

For DNA staining, cells were incubated with 10 µg/ml Hoechst 33258 for 10 min in the dark before imaging in the 4',6-diamidino-2-phenylindole (DAPI) channel as described (Wu et al., 2011).

Microscopy and data analysis

Strains were restreaked from −80°C stock and grown 1–2 d on yeast extract plus five supplements (YE5S) plates at 25°C. Cells were then inoculated and kept in exponential phase for ~48 h at 25°C except where noted. Before microscopy, cells were washed in Edinburgh minimal medium plus five supplements (EMM5S) twice to reduce autofluorescence and imaged on EMM5S with 20% gelatin pad with 5 µM n-propyl-gallate as described (Laporte et al., 2011; Ye et al.,

Strain	Genotype	Source/reference
JW81	h⁻ ade6-210 ura4-D18 leu1-32	Wu et al. (2003)
JW1063	h⁺ mYFP-cdc15 ade6-M216 leu1-32 ura4-D18	Wu and Pollard (2005)
JW1636	h⁺ mid1-6 ade6-M210 leu1-32 ura4-D18	Coffman et al. (2013)
JW1743	cdc15-140 ade6-M210 leu1-32 ura4-D18	Coffman et al. (2013)
JW1824	h⁺ klp8Δ::kanMX4 ade6 leu1-32 ura4-D18	Kim et al. (2010)
JW1825	h⁺ blt1Δ::kanMX4 ade6-M216 leu1-32 ura4-D18	Ye et al. (2012)
JW1826	h⁺ gef2Δ::kanMX4 ade6 leu1-32 ura4-D18	Ye et al. (2012)
JW2249	rng2-346 ade6-M210 leu1-32 ura4-D18	This study
JW2255	h⁺ mid1-366 ade6-M210 leu1-32 ura4-D18	Ye et al. (2012)
JW2854	h⁺ gef2Δ::hphMX6 ade6 leu1-32 ura4-D18	This study
JW2937	cdc15-140 gef2Δ::kanMX4 ade6 leu1-32 ura4-D18	This study
JW2972	h⁺ cdc11-136 gef2Δ::hphMX6 ade6 leu1-32 ura4-D18	Ye et al. (2012)
JW3009	gef2Δ::hphMX6 sid2-250 ade6 leu1-32 ura4-D18	Ye et al. (2012)
JW3021	gef2Δ::hphMX6 cdc7-24 ade6 leu1-32 ura4-D18	This study
JW3041	h⁺ rho4Δ::kanMX4 ade6 leu1-32 ura4-D18	Kim et al. (2010)
JW3078	h⁻ gef2Δ::hphMX6 plo1.ts18::ura4⁺ ade6 leu1-32 ura4-D18	Ye et al. (2012)
JW3204	h⁻ gef2-13Myc-hphMX6 ade6-M210 leu1-32 ura4-D18	Ye et al. (2012)
JW3325	gef2-13Myc-hphMX6 mYFP-cdc15 ade6-M210 leu1-32 ura4-D18	This study
JW3561	h⁻ kanMX6-3nmt1-gef2 ade6-M216 leu1-32 ura4-D18	This study
JW3562	h⁻ kanMX6-41nmt1-gef2 ade6-M216 leu1-32 ura4-D18	This study
JW3622	h⁺ gef2-13Myc-hphMX6 ade6-M210 leu1-32 ura4-D18	This study
JW3773	h⁻ nod1Δ::kanMX6 ade6-M210 leu1-32 ura4-D18	This study
JW3814	h⁺ nod1Δ::kanMX6 gef2Δ::kanMX4 ade6 leu1-32 ura4-D18	This study
JW3815	nod1Δ::kanMX6 plo1.ts18::ura4⁺ ade6-M210 ura4-D18 leu1-32	This study
JW3825	h⁻ kanMX6-Pgef2-mECitrine-4Gly-gef2 ade6-M216 leu1-32 ura4-D18	Ye et al. (2012)
JW3826	h⁻ kanMX6-Pgef2-mECitrine-4Gly-gef2-(957-1101) ade6-M216 leu1-32 ura4-D18	Ye et al. (2012)

TABLE 2: S. pombe strains used in this study.

Strain	Genotype	Source/reference
JW3861	h⁺ nod1Δ::kanMX6 mid1-6 ade6-M210 leu1-32 ura4-D18	This study
JW3873	nod1Δ::kanMX6 gef2Δ::kanMX4 plo1.ts18::ura4⁺ade6 leu1-32 ura4-D18	This study
JW3875	h⁻ nod1Δ::kanMX6 mid1-366 ade6-M210 leu1-32 ura4-D18	This study
JW4008	h⁻ nod1-mECitrine-kanMX6 ade6-M210 leu1-32 ura4-D18	This study
JW4010	h⁻ nod1-tdTomato-hphMX6 ade6-M210 leu1-32 ura4-D18	This study
JW4013	h⁻ nod1-13Myc-hphMX6 ade6-M210 leu1-32 ura4-D18	This study
JW4014	nod1Δ::kanMX6 kanMX6-Pgef2-mECitrine-4Gly-gef2 ade6 leu1-32 ura4-D18	This study
JW4015	h⁻ nod1Δ::kanMX6 cdc4-8 ade6 leu1-32 ura4-D18	This study
JW4016	h⁻ nod1Δ::kanMX6 cdc15-140 ade6-M210 leu1-32 ura4-D18	This study
JW4038	nod1-mECitrine-kanMX6 gef2Δ::hphMX6 ade6 leu1-32 ura4-D18	This study
JW4042	nod1Δ::kanMX6 rng2-D5 ade6-M210 leu1-32 ura4-D18	This study
JW4043	h⁺ nod1Δ::kanMX6 rng2-346 ade6-M210 leu1-32 ura4-D18	This study
JW4098	nod1Δ::kanMX6 cdr2Δ::kanMX6 ade6 leu1-32 ura4-D18	This study
JW4099	h⁺ nod1Δ::kanMX6 blt1Δ::kanMX4 ade6 leu1-32 ura4-D18	This study
JW4226	h⁺ kanMX6-Pgef2-tdTomato-4Gly-gef2 ade6-M210 leu1-32 ura4-D18	Ye et al. (2012)
JW4256	nod1-tdTomato-hphMX6 kanMX6-Pgef2-mECitrine-4Gly-gef2-(957-1101) ade6 leu1-32 ura4-D18	This study
JW4259	h⁻ nod1Δ::hphMX6 ade6-M210 leu1-32 ura4-D18	This study
JW4294	nod1Δ::hphMX6 sid2-250 ade6-M210 leu1-32 ura4-D18	This study
JW4295	klp8Δ::kanMX4 nod1Δ::hphMX6 ade6-M210 leu1-32 ura4-D18	This study
JW4304	nod1Δ::hphMX6 cdc7-24 ade6 leu1-32 ura4-D18 his2 or his7	This study
JW4306	nod1Δ::hphMX6 cdc11-136 ade6-M210 leu1-32 ura4-D18 his2 or his7	This study
JW4325	h⁻ nod1(1-209)-mECitrine-kanMX6 ade6-M210 leu1-32 ura4-D18	This study
JW4326	h⁻ nod1(1-328)-mECitrine-kanMX6 ade6-M210 leu1-32 ura4-D18	This study
JW4330	nod1-13Myc-hphMX6 kanMX6-Pgef2-mECitrine-4Gly-gef2 ade6 leu1-32 ura4-D18	This study
JW4331	nod1-13Myc-hphMX6 kanMX6-Pgef2-mECitrine-4Gly-gef2-(957-1101) ade6 leu1-32 ura4-D18	This study
JW4355	nod1-tdTomato-hphMX6 kanMX6-Pgef2-mECitrine-4Gly-gef2-(1-956)-TADH1-hphMX6 ade6 leu1-32 ura4-D18	This study
JW4359	h⁻ nod1(1-328)-mECitrine-kanMX6 kanMX6-Pgef2-tdTomato-4Gly-gef2 ade6 leu1-32 ura4-D18	This study
JW4453	h⁻ kanMX6-Pnod1-mECitrine-nod1 ade6-M210 leu1-32 ura4-D18	This study
JW4455	h⁻ kanMX6-Pnod1-mECitrine-nod1(329-419) ade6-M210 leu1-32 ura4-D18	This study
JW4457	nod1-mEGFP-hphMX6 kanMX6-Pgef2-tdTomato-4Gly-gef2 ade6-M210 leu1-32 ura4-D18	This study
JW4750	Pnod1-mECitrine-nod1 ade6-M210 leu1-32 ura4-D18	This study
JW4856	h⁺ Pnod1-mECitrine-nod1(329-419) ade6-M210 leu1-32 ura4-D18	This study
JW4909	rho4Δ::kanMX6 leu1::GFP-rho4 gef2Δ::kanMX4 leu1-32 ura4-D18 ade6	This study
JW4910	h⁻ rho4Δ::kanMX6 leu1::GFP-rho4 nod1Δ::kanMX6 leu1-32 ura4-D18	This study
JW4912	Pgef2-mECitrine-4Gly-gef2 ade6 leu1-32 ura4-D18	This study
JW5027	cdc15-140 nod1-mECitrine-kanMX6 gef2Δ::hphMX6 ade6 leu1-32 ura4-D18	This study
JW5028	cdc15-140 nod1-mECitrine-kanMX6 ade6-M210 leu1-32 ura4-D18	This study
JW5065	h⁺ Pnod1-mECitrine-nod1(210-419) ade6-M210 leu1-32 ura4-D18	This study
JW5093	kanMX6-Pnod1-mECitrine-nod1 gef2-13Myc-hphMX6 ade6-M210 leu1-32 ura4-D18	This study
JW5095	kanMX6-Pnod1-mECitrine-nod1(329-419) gef2-13Myc-hphMX6 ade6-M210 leu1-32 ura4-D18	This study
JW5107	kanMX6-Pgef2-tdTomato-4Gly-gef2 kanMX6-Pnod1-mECitrine-nod1(329-419) ade6-M210 leu1-32 ura4-D18	This study
JW5120	nod1-13Myc-hphMX6 mYFP-cdc15 ade6 leu1-32 ura4-D18	This study

TABLE 2: *S. pombe* strains used in this study. Continued

Strain	Genotype	Source/reference
JW5329	h^+ gef2Δ::kanMX4 cdc15-140 GFP-bgs1-leu1$^+$ bgs1Δ::ura4$^+$ rlc1-tdTomato-natMX6 ade6 leu1-32 ura4-D18	This study
JW5330	nod1Δ::kanMX6 cdc15-140 GFP-bgs1-leu1$^+$ bgs1Δ::ura4$^+$ rlc1-tdTomato-natMX6 ade6-M210 leu1-32 ura4-D18	This study
JW5357	h^- cdc15-140 GFP-bgs1-leu1$^+$ bgs1Δ::ura4$^+$ rlc1-tdTomato-natMX6 ade6-M210 leu1-32 ura4-D18	This study
JW5360	sid2-250 kanMX6-3nmt1-gef2 ade6 leu1-32 ura4-D18	This study
JW5361	sid2-250 kanMX6-41nmt1-gef2 ade6 leu1-32 ura4-D18	This study
JW5405	sid2-1 kanMX6-3nmt1-gef2 ade6 leu1-32 ura4-D18	This study
JW5406	sid2-1 kanMX6-41nmt1-gef2 ade6 leu1-32 ura4-D18	This study
JW5503	rho4Δ::kanMX4 cdc7-24 ade6 leu1-32 ura4-D18 his7-366	This study
JW5504	rho4Δ::kanMX4 cdc11-136 ade6 leu1-32 ura4-D18	This study
JW5505	rho4Δ::kanMX4 sid2-250 ade6 leu1-32 ura4-D18	This study
JW5580	gef2Δ::kanMX4 sid2-GFP-ura4$^+$ade6-M210 leu1-32 ura4-D18	This study
JW5581	nod1Δ::kanMX6 sid2-GFP-ura4$^+$ade6-M210 leu1-32 ura4-D18	This study
JW5582	Pgef2-mECitrine-4Gly-gef2 Pmyo2-mCFP-myo2 ade6 leu1-32 ura4-D18	This study
JW5583	cdc15-140 Pgef2-mECitrine-4Gly-gef2 Pmyo2-mCFP-myo2 ade6 leu1-32 ura4-D18	This study
IH1600	h^+ plo1.ts18::ura4$^+$ ura4-D18 leu1-32 ade6-M210 his2	MacIver et al. (2003)
JM578	h^+ cdr2Δ::kanMX6 ade6 leu1-32 ura4-D18	Moseley et al. (2009)
PPG1580	h^- rho4Δ::kanMX6 leu1::GFP-rho4 leu1-32 ura4-D18	Santos et al. (2003)
TP7	h^- cdc4-8 his7-366 leu1-32 ura4-D18 ade6-M216	Thomas Pollard (Yale University, New Haven, CT)
TP34	h^- cdc7-24 his7-366 leu1-32 ade6-M216 ura4-D18	Thomas Pollard
TP47	h^- cdc11-136 ura4-D18 leu1-32 his7-366	Bezanilla et al. (1997)
VS2367	h^+ sid2-1 ade6-M210 leu1-32 ura4-D18	Salimova et al. (2000)
YDM26	h^- rng2-D5 ade6-210 ura4-D18 leu1-32	Eng et al. (1998)
YDM415	h^- sid2-GFP-ura4$^+$ ade6-M210 leu1-32 ura4-D18	Sparks et al. (1999)
YDM429	h^+ sid2-250 ade6-M210 leu1-32 ura4-D18	Sparks et al. (1999)

TABLE 2: *S. pombe* strains used in this study. Continued

2012). For long movies, cells were washed in YE5S and resuspended in YE5S with 5 µM n-propyl-gallate. Then 2-µl concentrated cells were spotted onto a coverglass-bottom dish (Delta TPG Dish; Biotechs, Butler, PA) and covered with a layer of YE5S agar before imaging at 23.5°C or in a preheated climate chamber (stage top incubator INUB-PPZI2-F1 equipped with UNIV2-D35 dish holder; Tokai Hit, Shizuoka-ken, Japan) for imaging at the restrictive temperatures for certain mutants.

Microscopy was performed at 23.5–25°C except where noted. To visualize cell morphology, DNA, and septum, Hoechst-stained cells were imaged with a 100×/1.4 numeral aperture (NA) Plan-Apo objective lens on a Nikon Eclipse Ti inverted microscope (Nikon, Melville, NY) equipped with a Nikon cooled digital camera DS-Ql1 and a DAPI filter. Other experiments were performed using 100×/1.4 NA Plan-Apo objective lenses (Nikon) on a spinning disk confocal microscope (UltraVIEW ERS; PerkinElmer Life and Analytical Sciences, Waltham, MA) with 440- and 568-nm solid state lasers and 488- and 514-nm argon ion lasers and an ORCA-AG camera (Hamamatsu, Bridgewater, NJ) with 2 × 2 binning, or on a spinning disk confocal microscope (UltraVIEW Vox CSUX1 system, PerkinElmer Life and Analytical Sciences) with 440-, 488-, 515-, and 561-nm solid-state lasers and a back-thinned, electron-multiplying charge-coupled device camera (Hamamatsu C9100-13) without binning.

Images were analyzed using ImageJ (National Institutes of Health, Bethesda, MD), UltraVIEW, or Volocity (PerkinElmer) software. Fluorescence images shown in figures and movies are maximum projections of images stacks at 0.4- to 0.6-µm spacing except where noted. Nod1 and Gef2 molecules in cells were counted globally or locally by measuring fluorescence intensity as described (Laporte et al., 2011). Briefly, tagged Nod1 or Gef2 cells were mixed with wt cells and imaged with 11 z-sections with 0.4-µm spacing on the UltraVIEW ERS confocal system. The offset was subtracted from images that were then corrected for uneven illumination. Mean intensity in whole cells was measured in sum intensity projections and subtracted by that of wt cells as background. Mean intensity in the mature contractile ring was measured using the polygon region of interest (ROI) tool in ImageJ on a sum intensity projection. A ≥3× larger ROI that included the contractile ring was chosen for calculation of background intensity after subtracting ring intensity. For nodes, the fluorescence intensity was measured using a circular ROI with a diameter of five pixels that covered the whole node at the best focal plan. The intensity near the plasma membrane outside of the broad band of nodes was used for background subtraction to

avoid overlapping with other nodes. The global and local intensities of Nod1 and Gef2 were then normalized to molecule numbers using previous Gef2 data as a reference (Wu and Pollard, 2005; Wu et al., 2008; Ye et al., 2012)

FRAP analysis

FRAP assays were performed using the photokinesis unit on the UltraVIEW Vox confocal system, similar to the assays described before (Coffman et al., 2009; Laporte et al., 2011). The best focal plane for bleaching was chosen from z-stacks. Selected ROIs were bleached to <50% of the original fluorescence intensity after five prebleach images were collected. One hundred postbleach images with 10-s delay were collected. The images were then corrected for background and photobleaching during image acquisition at nonbleached sites. We normalized prebleach intensity of the ROI to 100%, the intensity just after bleaching to 0%, and the end of the bleach time as time 0. Intensity of every three consecutive postbleaching time points was averaged to reduce noise. The data were then plotted and fitted using the exponential equation $y = m_1 + m_2 \exp(-m_3 x)$, where m_3 is the off-rate (KaleidaGraph; Synergy Software, Reading, PA). The half-time of recovery was calculated as $t_{1/2} = (\ln 2)/m_3$. The p values in this study were calculated using two-tailed Student's t tests.

IP and Western blotting

IP assay and Western blotting were carried out as previously described (Laporte et al., 2011; Lee and Wu, 2012). Briefly, mECitrine-tagged proteins were pulled down from fission yeast cell extract by protein G covalently coupled magnetic Dynabeads (100.04D; Invitrogen, Carlsbad, CA) with polyclonal anti-GFP antibodies (NB600-308; Novus Biologicals, Littleton, CO). The bead samples were then boiled in sample buffer after washing three times. The protein samples were then separated in SDS–PAGE, and Western blotting was performed using monoclonal anti-GFP antibody (11814460001, 1:2000 dilution; Roche, Mannheim, Germany) or monoclonal anti-Myc antibody (9E10, 1:5000 dilution; Santa Cruz Biotechnology, Santa Cruz, CA). The anti-tubulin monoclonal TAT1 antibody was used at 1:20,000 dilution (Woods et al., 1989). Anti-mouse secondary antibody was used at 1:5000 dilution.

Yeast two-hybrid assays

β-Galactosidase activity assays were performed to semiquantitatively detect protein interactions in yeast two-hybrid assays (Laporte et al., 2011). DNAs or cDNAs of interest were constructed into vectors with either VP16 activation domain or GBT9 DNA-binding domain. The pairs of plasmids were then cotransformed into Saccharomyces cerevisiae strain MAV203 (11281-011; Invitrogen) and plated on solid medium lacking leucine and tryptophan (SD-L-W). The transformants were selected and used for β-galactosidase activity measurements in the o-nitrophenyl β-D-galactopyranoside assay (Sigma-Aldrich, St. Louis, MO). The results are displayed as fold changes over the highest negative control value.

Protein purification and the interaction between Gef2 and Rho GTPases

Pull-down assays between recombinant 6His-Gef2 (GEF) and GST-Rho proteins were adapted from a previous study (Iwaki et al., 2003). Expression of 6His-tagged GEF domain of Gef2 (aa 211–600) was induced when ArcticExpress RIL cells (230193; Agilent Technologies, Santa Clara, CA) carrying the plasmid were grown at 10°C for 18 h after adding 1 mM isopropyl-β-D-thiogalactoside (IPTG; Saha and Pollard, 2012b). After sonication (output 9, 50% duty cycle,

4× 20 pulses) and ultracentrifugation (25,000 rpm for 15 min, then 38,000 rpm for 30 min), 6His-Gef2 (GEF) was purified on Talon Metal Affinity Resin (635501; Clontech, Mountain View, CA) followed by gel filtration with a HiLoad 16×60 Superdex 200 (17-5175-01; GE Healthcare, Buckinghamshire, United Kingdom) in phosphate buffer (50 mM sodium phosphate, pH 6.2, 0.3 M NaCl, 1 mM dithiothreitol [DTT]). The purified His-Gef2 (GEF) was then dialyzed into the final binding buffer (25 mM 3-(N-morpholino)propanesulfonic acid, pH 7.2, 60 mM β-glycerophosphate, 15 mM p-nitrophenyl phosphate, 1 mM DTT, 1% Triton X-100, 1 mM phenylmethylsulfonyl fluoride, and protease inhibitor tablets). GST and GST-Rho1 to Rho5 and Cdc42 were purified from BL21(DE3)pLysS cells (69451; Novagen, EMD Chemicals, Darmstadt, Germany; induced with 0.5 mM IPTG at 15°C for 6 h) using glutathione–Sepharose beads (17-5132-01; GE Healthcare). The beads with Rho proteins were then incubated at 30°C for 10 min with buffer containing 50 mM Tris (pH 7.5), 1 mM DTT, and 5 mM EDTA to deplete nucleotides. Then 500 μl of 0.25 μM 6His-Gef2 (GEF) in binding buffer was added to 30 μl of beads with each nucleotide-depleted Rho protein and incubated at 4°C for 1 h. After incubation, glutathione beads were washed with 1 ml of binding buffer three times, and the bound proteins were detect by Western blotting. Rho GTPases were detected by monoclonal anti-GST antibody (3G10/1B3, 1:5000 dilution; NB600-446, Novus Biologicals), and bound 6His-Gef2 (GEF) was detected by anti-His antibody (631212, 1:10,000 dilution; Clontech). Secondary anti-mouse antibody was used at 1:5000 dilution.

REFERENCES

Almonacid M, Celton-Morizur S, Jakubowski JL, Dingli F, Loew D, Mayeux A, Chen JS, Gould KL, Clifford DM, Paoletti A (2011). Temporal control of contractile ring assembly by Plo1 regulation of myosin II recruitment by Mid1/anillin. Curr Biol 21, 473–479.

Almonacid M, Moseley JB, Janvore J, Mayeux A, Fraisier V, Nurse P, Paoletti A (2009). Spatial control of cytokinesis by Cdr2 kinase and Mid1/anillin nuclear export. Curr Biol 19, 961–966.

Arasada R, Pollard TD (2011). Distinct roles for F-BAR proteins Cdc15p and Bzz1p in actin polymerization at sites of endocytosis in fission yeast. Curr Biol 21, 1450–1459.

Arellano M, Duran A, Pérez P (1997). Localisation of the Schizosaccharomyces pombe rho1p GTPase and its involvement in the organisation of the actin cytoskeleton. J Cell Sci 110, 2547–2555.

Bähler J, Steever AB, Wheatley S, Wang Y-L, Pringle JR, Gould KL, McCollum D (1998a). Role of polo kinase and Mid1p in determining the site of cell division in fission yeast. J Cell Biol 143, 1603–1616.

Bähler J, Wu J-Q, Longtine MS, Shah NG, McKenzie A III, Steever AB, Wach A, Philippsen P, Pringle JR (1998b). Heterologous modules for efficient and versatile PCR-based gene targeting in Schizosaccharomyces pombe. Yeast 14, 943–951.

Balasubramanian MK, McCollum D, Chang L, Wong KC, Naqvi NI, He X, Sazer S, Gould KL (1998). Isolation and characterization of new fission yeast cytokinesis mutants. Genetics 149, 1265–1275.

Bement WM, Benink HA, von Dassow G (2005). A microtubule-dependent zone of active RhoA during cleavage plane specification. J Cell Biol 170, 91–101.

Bezanilla M, Forsburg SL, Pollard TD (1997). Identification of a second myosin-II in *Schizosaccharomyces pombe*: Myp2p is conditionally required for cytokinesis. Mol Biol Cell 8, 2693–2705.

Bi E, Park H-O (2012). Cell polarization and cytokinesis in budding yeast. Genetics 191, 347–387.

Butty AC, Perrinjaquet N, Petit A, Jaquenoud M, Segall JE, Hofmann K, Zwahlen C, Peter M (2002). A positive feedback loop stabilizes the guanine-nucleotide exchange factor Cdc24 at sites of polarization. EMBO J 21, 1565–1576.

Calonge TM, Nakano K, Arellano M, Arai R, Katayama S, Toda T, Mabuchi I, Pérez P (2000). *Schizosaccharomyces pombe* Rho2p GTPase regulates cell wall α-glucan biosynthesis through the protein kinase Pck2p. Mol Biol Cell 11, 4393–4401.

Carnahan RH, Gould KL (2003). The PCH family protein, Cdc15p, recruits two F-actin nucleation pathways to coordinate cytokinetic actin ring formation in *Schizosaccharomyces pombe*. J Cell Biol 162, 851–862.

Cerutti L, Simanis V (1999). Asymmetry of the spindle pole bodies and spg1p GAP segregation during mitosis in fission yeast. J Cell Sci 112, 2313–2321.

Chang F, Wollard A, Nurse P (1996). Isolation and characterization of fission yeast mutants defective in the assembly and placement of the contractile actin ring. J Cell Sci 109, 131–142.

Chang L, Gould KL (2000). Sid4p is required to localize components of the septation initiation pathway to the spindle pole body in fission yeast. Proc Natl Acad Sci USA 97, 5249–5254.

Chen C-T, Feoktistova A, Chen JS, Shim YS, Clifford DM, Gould KL, McCollum D (2008). The SIN kinase Sid2 regulates cytoplasmic retention of the *S. pombe* Cdc14-like phosphatase Clp1. Curr Biol 18, 1594–1599.

Chen Q, Pollard TD (2011). Actin filament severing by cofilin is more important for assembly than constriction of the cytokinetic contractile ring. J Cell Biol 195, 485–498.

Coffman VC, Nile AH, Lee I-J, Liu HY, Wu J-Q (2009). Roles of formin nodes and myosin motor activity in Mid1p-dependent contractile-ring assembly during fission yeast cytokinesis. Mol Biol Cell 20, 5195–5210.

Coffman VC, Sees JA, Kovar DR, Wu J-Q (2013). The formins Cdc12 and For3 cooperate during contractile-ring assembly in cytokinesis. J Cell Biol (*in press*).

Coll PM, Trillo Y, Ametzazurra A, Pérez P (2003). Gef1p, a new guanine nucleotide exchange factor for Cdc42p, regulates polarity in *Schizosaccharomyces pombe*. Mol Biol Cell 14, 313–323.

Deng L, Moseley JB (2013). Compartmentalized nodes control mitotic entry signaling in fission yeast. Mol Biol Cell 24, 1872–1881.

Eng K, Naqvi NI, Wong KC, Balasubramanian MK (1998). Rng2p, a protein required for cytokinesis in fission yeast, is a component of the actomyosin ring and the spindle pole body. Curr Biol 8, 611–621.

Fankhauser C, Reymond A, Cerutti L, Utzig S, Hofmann K, Simanis V (1995). The *S. pombe cdc15* gene is a key element in the reorganization of F-actin at mitosis. Cell 82, 435–444.

Fankhauser C, Simanis V (1993). The *Schizosaccharomyces pombe cdc14* gene is required for septum formation and can also inhibit nuclear division. Mol Biol Cell 4, 531–539.

Fankhauser C, Simanis V (1994). The *cdc7* protein kinase is a dosage dependent regulator of septum formation in fission yeast. EMBO J 13, 3011–3019.

Furge KA, Cheng Q-C, Jwa M, Shin S, Song K, Albright CF (1999). Regions of Byr4, a regulator of septation in fission yeast, that bind Spg1 or Cdc16 and form a two-component GTPase-activating protein with Cdc16. J Biol Chem 274, 11339–11343.

Furge KA, Wong K, Armstrong J, Balasubramanian M, Albright CF (1998). Byr4 and Cdc16 form a two-component GTPase-activating protein for the Spg1 GTPase that controls septation in fission yeast. Curr Biol 8, 947–954.

García P, García I, Marcos F, de Garibay GR, Sánchez Y (2009). Fission yeast rgf2p is a rho1p guanine nucleotide exchange factor required for spore wall maturation and for the maintenance of cell integrity in the absence of rgf1p. Genetics 181, 1321–1334.

García P, Tajadura V, García I, Sánchez Y (2006a). Rgf1p is a specific Rho1-GEF that coordinates cell polarization with cell wall biogenesis in fission yeast. Mol Biol Cell 17, 1620–1631.

García P, Tajadura V, García I, Sánchez Y (2006b). Role of Rho GTPases and Rho-GEFs in the regulation of cell shape and integrity in fission yeast. Yeast 23, 1031–1043.

Goyal A, Simanis V (2012). Characterization of *ypa1* and *ypa2*, the *Schizosaccharomyces pombe* orthologs of the peptidyl proyl isomerases that activate PP2A, reveals a role for Ypa2p in the regulation of cytokinesis. Genetics 190, 1235–1250.

Green RA, Paluch E, Oegema K (2012). Cytokinesis in animal cells. Annu Rev Cell Dev Biol 28, 29–58.

Guertin DA, Chang L, Irshad F, Gould KL, McCollum D (2000). The role of the Sid1p kinase and Cdc14p in regulating the onset of cytokinesis in fission yeast. EMBO J 19, 1803–1815.

Guzman-Vendrell M, Baldissard S, Almonacid M, Mayeux A, Paoletti A, Moseley JB (2013). Blt1 and Mid1 provide overlapping membrane anchors to position the division plane in fission yeast. Mol Cell Biol 33, 418–428.

Hachet O, Berthelot-Grosjean M, Kokkoris K, Vincenzetti V, Moosbrugger J, Martin SG (2011). A phosphorylation cycle shapes gradients of the DYRK family kinase Pom1 at the plasma membrane. Cell 145, 1116–1128.

Hachet O, Simanis V (2008). Mid1p/anillin and the septation initiation network orchestrate contractile ring assembly for cytokinesis. Genes Dev 22, 3205–3216.

Hirota K, Tanaka K, Ohta K, Yamamoto M (2003). Gef1p and Scd1p, the Two GDP-GTP exchange factors for Cdc42p, form a ring structure that shrinks during cytokinesis in *Schizosaccharomyces pombe*. Mol Biol Cell 14, 3617–3627.

Hou M-C, Salek J, McCollum D (2000). Mob1p interacts with the Sid2p kinase and is required for cytokinesis in fission yeast. Curr Biol 10, 619–622.

Huang Y, Yan H, Balasubramanian MK (2008). Assembly of normal actomyosin rings in the absence of Mid1p and cortical nodes in fission yeast. J Cell Biol 183, 979–988.

Imamura H, Tanaka K, Hihara T, Umikawa M, Kamei T, Takahashi K, Sasaki T, Takai Y (1997). Bni1p and Bnr1p: downstream targets of the Rho family small G-proteins which interact with profilin and regulate actin cytoskeleton in *Saccharomyces cerevisiae*. EMBO J 16, 2745–2755.

Iwaki N, Karatsu K, Miyamoto M (2003). Role of guanine nucleotide exchange factors for Rho family GTPases in the regulation of cell morphology and actin cytoskeleton in fission yeast. Biochem Biophys Res Commun 312, 414–420.

Jiang W, Hallberg RL (2001). Correct regulation of the septation initiation network in *Schizosaccharomyces pombe* requires the activities of *par1* and *par2*. Genetics 158, 1413–1429.

Jin Q-W, McCollum D (2003). Scw1p antagonizes the septation initiation network to regulate septum formation and cell separation in the fission yeast *Schizosaccharomyces pombe*. Eukaryot Cell 2, 510–520.

Jin Q-W, Zhou M, Bimbo A, Balasubramanian MK, McCollum D (2006). A role for the septation initiation network in septum assembly revealed by genetic analysis of *sid2–250* suppressors. Genetics 172, 2101–2112.

Johnson AE, McCollum D, Gould KL (2012). Polar opposites: fine-tuning cytokinesis through SIN asymmetry. Cytoskeleton (Hoboken) 69, 686–699.

Jones DT (1999). Protein secondary structure prediction based on position-specific scoring matrices. J Mol Biol 292, 195–202.

Jourdain I, Brzezinska EA, Toda T (2013). Fission yeast Nod1 is a component of cortical nodes involved in cell size control and division site placement. PLoS One 8, e54142.

Jwa M, Song K (1998). Byr4, a dosage-dependent regulator of cytokinesis in *S. pombe*, interacts with a possible small GTPase pathway including Spg1 and Cdc16. Mol Cells 8, 240–245.

Kim DU *et al.* (2010). Analysis of a genome-wide set of gene deletions in the fission yeast *Schizosaccharomyces pombe*. Nat Biotechnol 28, 617–623.

Kita A, Li C, Yu Y, Umeda N, Doi A, Yasuda M, Ishiwata S, Taga A, Horiuchi Y, Sugiura R (2011). Role of the small GTPase Rho3 in Golgi/endosome trafficking through functional interaction with adaptin in fission yeast. PLoS One 6, e16842.

Kovar DR, Kuhn JR, Tichy AL, Pollard TD (2003). The fission yeast cytokinesis formin Cdc12p is a barbed end actin filament capping protein gated by profilin. J Cell Biol 161, 875–887.

Krapp A, Collin P, Cano Del Rosario E, Simanis V (2008). Homoeostasis between the GTPase Spg1p and its GAP in the regulation of cytokinesis in *S. pombe*. J Cell Sci 121, 601–608.

Krapp A, Schmidt S, Cano E, Simanis V (2001). *S. pombe* cdc11p, together with sid4p, provides an anchor for septation initiation network proteins on the spindle pole body. Curr Biol 11, 1559–1568.

Krapp A, Simanis V (2008). An overview of the fission yeast septation initiation network (SIN). Biochem Soc Trans 36, 411–415.

Laporte D, Coffman VC, Lee I-J, Wu J-Q (2011). Assembly and architecture of precursor nodes during fission yeast cytokinesis. J Cell Biol 192, 1005–1021.

Laporte D, Ojkic N, Vavylonis D, Wu J-Q (2012). α-Actinin and fimbrin cooperate with myosin II to organize actomyosin bundles during contractile-ring assembly. Mol Biol Cell 23, 3094–3110.

Lee I-J, Coffman VC, Wu J-Q (2012). Contractile-ring assembly in fission yeast cytokinesis: Recent advances and new perspectives. Cytoskeleton (Hoboken) 69, 751–763.

Lee I-J, Wu J-Q (2012). Characterization of Mid1 domains for targeting and scaffolding in fission yeast cytokinesis. J Cell Sci 125, 2973–2985.

Lehner CF ((1992). The *pebble* gene is required for cytokinesis in *Drosophila*. J Cell Sci 103, 1021–1030.

MacIver FH, Tanaka K, Robertson AM, Hagan IM (2003). Physical and functional interactions between polo kinase and the spindle pole component Cut12 regulate mitotic commitment in *S. pombe*. Genes Dev 17, 1507–1523.

Mana-Capelli S, McLean JR, Chen C-T, Gould KL, McCollum D (2012). The kinesin-14 Klp2 is negatively regulated by the SIN for proper spindle elongation and telophase nuclear positioning. Mol Biol Cell 23, 4592–4600.

Martin SG, Berthelot-Grosjean M (2009). Polar gradients of the DYRK-family kinase Pom1 couple cell length with the cell cycle. Nature 459, 852–856.

Maundrell K (1990). *nmt1* of fission yeast. A highly transcribed gene completely repressed by thiamine. J Biol Chem 265, 10857–10864.

Mehta S, Gould KL (2006). Identification of functional domains within the septation initiation network kinase, Cdc7. J Biol Chem 281, 9935–9941.

Moreno S, Klar A, Nurse P (1991). Molecular genetic analysis of fission yeast *Schizosaccharomyces pombe*. Methods Enzymol 194, 795–823.

Morrell-Falvey JL, Ren L, Feoktistova A, Haese GD, Gould KL (2005). Cell wall remodeling at the fission yeast cell division site requires the Rho-GEF Rgf3p. J Cell Sci 118, 5563–5573.

Morrell JL et al. (2004). Sid4p-Cdc11p assembles the septation initiation network and its regulators at the *S. pombe* SPB. Curr Biol 14, 579–584.

Moseley JB, Mayeux A, Paoletti A, Nurse P (2009). A spatial gradient coordinates cell size and mitotic entry in fission yeast. Nature 459, 857–860.

Motegi F, Mishra M, Balasubramanian MK, Mabuchi I (2004). Myosin-II reorganization during mitosis is controlled temporally by its dephosphorylation and spatially by Mid1 in fission yeast. J Cell Biol 165, 685–695.

Mutoh T, Nakano K, Mabuchi I (2005). Rho1-GEFs Rgf1 and Rgf2 are involved in formation of cell wall and septum, while Rgf3 is involved in cytokinesis in fission yeast. Genes Cells 10, 1189–1202.

Nakano K, Arai R, Mabuchi I (1997). The small GTP-binding protein Rho1 is a multifunctional protein that regulates actin localization, cell polarity, and septum formation in the fission yeast *Schizosaccharomyces pombe*. Genes Cells 2, 679–694.

Nakano K, Arai R, Mabuchi I (2005). Small GTPase Rho5 is a functional homologue of Rho1, which controls cell shape and septation in fission yeast. FEBS Lett 579, 5181–5186.

Nakano K, Imai J, Arai R, Toh EA, Matsui Y, Mabuchi I (2002). The small GTPase Rho3 and the diaphanous/formin For3 function in polarized cell growth in fission yeast. J Cell Sci 115, 4629–4639.

Nakano K, Mutoh T, Arai R, Mabuchi I (2003). The small GTPase Rho4 is involved in controlling cell morphology and septation in fission yeast. Genes Cells 8, 357–370.

Nishimura Y, Yonemura S (2006). Centralspindlin regulates ECT2 and RhoA accumulation at the equatorial cortex during cytokinesis. J Cell Sci 119, 104–114.

O'Keefe L, Somers WG, Harley A, Saint R (2001). The pebble GTP exchange factor and the control of cytokinesis. Cell Struct Funct 26, 619–626.

Ojkic N, Wu J-Q, Vavylonis D (2011). Model of myosin node aggregation into a contractile ring: the effect of local alignment. J Phys Condens Matter 23, 374103.

Padmanabhan A, Bakka K, Sevugan M, Naqvi NI, D'Souza V, Tang X, Mishra M, Balasubramanian MK (2011). IQGAP-related Rng2p organizes cortical nodes and ensures position of cell division in fission yeast. Curr Biol 21, 467–472.

Paoletti A, Chang F (2000). Analysis of mid1p, a protein required for placement of the cell division site, reveals a link between the nucleus and the cell surface in fission yeast. Mol Biol Cell 11, 2757–2773.

Pérez P, Rincón SA (2010). Rho GTPases: regulation of cell polarity and growth in yeasts. Biochem J 426, 243–253.

Piekny A, Werner M, Glotzer M (2005). Cytokinesis: welcome to the Rho zone. Trends Cell Biol 15, 651–658.

Pinar M, Coll PM, Rincón SA, Pérez P (2008). *Schizosaccharomyces pombe* Pxl1 is a paxillin homologue that modulates Rho1 activity and participates in cytokinesis. Mol Biol Cell 19, 1727–1738.

Pollard TD, Wu J-Q (2010). Understanding cytokinesis: lessons from fission yeast. Nat Rev Mol Cell Biol 11, 149–155.

Proctor SA, Minc N, Boudaoud A, Chang F (2012). Contributions of turgor pressure, the contractile ring, and septum assembly to forces in cytokinesis in fission yeast. Curr Biol 22, 1601–1608.

Rincón S, Coll PM, Pérez P (2007). Spatial regulation of Cdc42 during cytokinesis. Cell Cycle 6, 1687–1691.

Rincón SA, Santos B, Pérez P (2006). Fission yeast Rho5p GTPase is a functional paralogue of Rho1p that plays a role in survival of spores and stationary-phase cells. Eukaryot Cell 5, 435–446.

Roberts-Galbraith RH, Chen J-S, Wang J, Gould KL (2009). The SH3 domains of two PCH family members cooperate in assembly of the *Schizosaccharomyces pombe* contractile ring. J Cell Biol 184, 113–127.

Roberts-Galbraith RH, Gould KL (2008). Stepping into the ring: the SIN takes on contractile ring assembly. Genes Dev 22, 3082–3088.

Roberts-Galbraith RH, Ohi MD, Ballif BA, Chen J-S, McLeod I, McDonald WH, Gygi SP, Yates JR III, Gould KL (2010). Dephosphorylation of F-BAR protein Cdc15 modulates its conformation and stimulates its scaffolding activity at the cell division site. Mol Cell 39, 86–99.

Saha S, Pollard TD (2012a). Anillin-related Mid1p coordinates the assembly of the cytokinetic contractile ring in fission yeast. Mol Biol Cell 23, 3982–3992.

Saha S, Pollard TD (2012b). Characterization of structural and functional domains of the anillin-related protein Mid1p that contribute to cytokinesis in fission yeast. Mol Biol Cell 23, 3993–4007.

Salimova E, Sohrmann M, Fournier N, Simanis V (2000). The *S. pombe* orthologue of the *S. cerevisiae mob1* gene is essential and functions in signalling the onset of septum formation. J Cell Sci 113, 1695–1704.

Santos B, Gutierrez J, Calonge TM, Pérez P (2003). Novel Rho GTPase involved in cytokinesis and cell wall integrity in the fission yeast *Schizosaccharomyces pombe*. Eukaryot Cell 2, 521–533.

Santos B, Martin-Cuadrado AB, Vazquez de Aldana CR, del Rey F, Pérez P (2005). Rho4 GTPase is involved in secretion of glucanases during fission yeast cytokinesis. Eukaryot Cell 4, 1639–1645.

Schmidt S, Sohrmann M, Hofmann K, Woollard A, Simanis V (1997). The Spg1p GTPase is an essential, dosage-dependent inducer of septum formation in *Schizosaccharomyces pombe*. Genes Dev 11, 1519–1534.

Slaughter BD, Smith SE, Li R (2009). Symmetry breaking in the life cycle of the budding yeast. Cold Spring Harb Perspect Biol 1, a003384.

Sohrmann M, Fankhauser C, Brodbeck C, Simanis V (1996). The *dmf1/mid1* gene is essential for correct positioning of the division septum in fission yeast. Genes Dev 10, 2707–2719.

Sparks CA, Morphew M, McCollum D (1999). Sid2p, a spindle pole body kinase that regulates the onset of cytokinesis. J Cell Biol 146, 777–790.

Su K-C, Takaki T, Petronczki M (2011). Targeting of the RhoGEF Ect2 to the equatorial membrane controls cleavage furrow formation during cytokinesis. Dev Cell 21, 1104–1115.

Tajadura V, García B, García I, García P, Sánchez Y (2004). *Schizosaccharomyces pombe* Rgf3p is a specific Rho1 GEF that regulates cell wall β-glucan biosynthesis through the GTPase Rho1p. J Cell Sci 117, 6163–6174.

Tanaka K, Petersen J, MacIver F, Mulvihill DP, Glover DM, Hagan IM (2001). The role of Plo1 kinase in mitotic commitment and septation in *Schizosaccharomyces pombe*. EMBO J 20, 1259–1270.

Tebbs IR, Pollard TD (2013). Separate roles of IQGAP Rng2p in forming and constricting the *Schizosaccharomyces pombe* cytokinetic contractile ring. Mol Biol Cell 24, 1904–1917.

Tolliday N, VerPlank L, Li R (2002). Rho1 directs formin-mediated actin ring assembly during budding yeast cytokinesis. Curr Biol 12, 1864–1870.

Tomlin GC, Morrell JL, Gould KL (2002). The spindle pole body protein Cdc11p links Sid4p to the fission yeast septation initiation network. Mol Biol Cell 13, 1203–1214.

Vavylonis D, Wu J-Q, Hao S, O'Shaughnessy B, Pollard TD (2008). Assembly mechanism of the contractile ring for cytokinesis by fission yeast. Science 319, 97–100.

Wachtler V, Huang Y, Karagiannis J, Balasubramanian MK (2006). Cell cycle-dependent roles for the FCH-domain protein Cdc15p in formation of the actomyosin ring in *Schizosaccharomyces pombe*. Mol Biol Cell 17, 3254–3266.

Wang H, Tang X, Balasubramanian MK (2003). Rho3p regulates cell separation by modulating exocyst function in *Schizosaccharomyces pombe*. Genetics 164, 1323–1331.

Watanabe S, Okawa K, Miki T, Sakamoto S, Morinaga T, Segawa K, Arakawa T, Kinoshita M, Ishizaki T, Narumiya S (2010). Rho and anillin-dependent control of mDia2 localization and function in cytokinesis. Mol Biol Cell 21, 3193–3204.

Wloka C, Bi E (2012). Mechanisms of cytokinesis in budding yeast. Cytoskeleton (Hoboken) 69, 710–726.

Wood V et al. (2012). PomBase: a comprehensive online resource for fission yeast. Nucleic Acids Res 40, D695–D699.

Woods A, Sherwin T, Sasse R, MacRae TH, Baines AJ, Gull K (1989). Definition of individual components within the cytoskeleton of Trypanosoma brucei by a library of monoclonal antibodies. J Cell Sci 93, 491–500.

Wu J-Q, Kuhn JR, Kovar DR, Pollard TD (2003). Spatial and temporal pathway for assembly and constriction of the contractile ring in fission yeast cytokinesis. Dev Cell 5, 723–734.

Wu J-Q, McCormick C, Pollard TD (2008). Counting proteins in living cells by quantitative fluorescence microscopy with internal standards. Methods Cell Biol 89, 253–273.

Wu J-Q, Pollard TD (2005). Counting cytokinesis proteins globally and locally in fission yeast. Science 310, 310–314.

Wu J-Q, Sirotkin V, Kovar DR, Lord M, Beltzner CC, Kuhn JR, Pollard TD (2006). Assembly of the cytokinetic contractile ring from a broad band of nodes in fission yeast. J Cell Biol 174, 391–402.

Wu J-Q, Ye Y, Wang N, Pollard TD, Pringle JR (2010). Cooperation between the septins and the actomyosin ring and role of a cell-integrity pathway during cell division in fission yeast. Genetics 186, 897–915.

Wu P, Zhao R, Ye Y, Wu J-Q (2011). Roles of the DYRK kinase Pom2 in cytokinesis, mitochondrial morphology, and sporulation in fission yeast. PLoS One 6, e28000.

Ye Y, Lee I-J, Runge KW, Wu J-Q (2012). Roles of putative Rho-GEF Gef2 in division-site positioning and contractile-ring function in fission yeast cytokinesis. Mol Biol Cell 23, 1181–1195.

Yoshida S, Kono K, Lowery DM, Bartolini S, Yaffe MB, Ohya Y, Pellman D (2006). Polo like kinase Cdc5 controls the local activation of Rho1 to promote cytokinesis. Science 313, 108–111.

Yuce O, Piekny A, Glotzer M (2005). An ECT2-centralspindlin complex regulates the localization and function of RhoA. J Cell Biol 170, 571–582.